ANESTHESIOLOGY

A Neural Circuit from the Paraventricular Thalamus to the Bed Nucleus of the Stria Terminalis for the Regulation of States of Consciousness during Sevoflurane Anesthesia in Mice

Jia-Yan Li, M.D., Ph.D., Shao-Jie Gao, M.M., Ran-Ran Li, Ph.D., Wei Wang, Ph.D., Jia Sun, M.M., Long-Qing Zhang, M.M., Jia-Yi Wu, M.M., Dai-Qiang Liu, M.D., Ph.D., Pei Zhang, Ph.D., Bo Tian, M.D., Ph.D., Wei Mei, M.D., Ph.D.

ANESTHESIOLOGY 2022; 136:709–31

EDITOR'S PERSPECTIVE

What We Already Know about This Topic

- The paraventricular thalamus plays a critical role in the maintenance of wakefulness
- The contribution of the paraventricular thalamus to mediating anesthesia mechanisms of actions is incompletely understood

What This Article Tells Us That Is New

- Chemogenetic inhibition of paraventricular glutamatergic neurons in the mouse thalamus projecting to the bed nucleus of the stria terminalis reduced induction time and prolonged emergence from sevoflurane anesthesia, while activation of this pathway had opposite effects
- These observations suggest that glutamatergic neurons of the paraventricular thalamus contribute to the mechanisms of actions of sevoflurane anesthesia *via* their projections to the bed nucleus of the stria terminalis

ABSTRACT

Background: The neural circuitry underlying sevoflurane-induced modulation of consciousness is poorly understood. This study hypothesized that the paraventricular thalamus bed nucleus of the stria terminalis pathway plays an important role in regulating states of consciousness during sevoflurane anesthesia.

Methods: Rabies virus–based transsynaptic tracing techniques were employed to reveal the neural pathway from the paraventricular thalamus to the bed nucleus of the stria terminalis. This study investigated the role of this pathway in sevoflurane anesthesia induction, maintenance, and emergence using chemogenetic and optogenetic methods combined with cortical electroencephalogram recordings. Both male and female mice were used in this study.

Results: Both γ-aminobutyric acid–mediated and glutamatergic neurons in the bed nucleus of the stria terminalis receive paraventricular thalamus glutamatergic projections. Chemogenetic inhibition of paraventricular thalamus glutamatergic neurons prolonged the sevoflurane anesthesia emergence time (mean ± SD, hM4D–clozapine *N*-oxide *vs.* mCherry–clozapine *N*-oxide, 281 ± 88 *vs.* 172 ± 48 s, $P < 0.001$, n = 24) and decreased the induction time (101 ± 32 *vs.* 136 ± 34 s, $P = 0.002$, n = 24), as well as the EC_{50} for the loss or recovery of the righting reflex under sevoflurane anesthesia (mean [95% CI] for the concentration at which 50% of the mice lost their righting reflex, 1.16 [1.12 to 1.20] *vs.* 1.49 [1.46 to 1.53] vol%, $P < 0.001$, n = 20; and for the concentration at which 50% of the mice recovered their righting reflex, 0.95 [0.86 to 1.03] *vs.* 1.34 [1.29 to 1.40] vol%, $P < 0.001$, n = 20). Similar results were observed during suppression of the paraventricular thalamus bed nucleus–stria terminalis pathway. Optogenetic activation of this pathway produced the opposite effects. Additionally, transient stimulation of this pathway efficiently induced behavioral arousal during continuous steady-state general anesthesia with sevoflurane and reduced the depth of anesthesia during sevoflurane-induced burst suppression.

Conclusions: In mice, axonal projections from the paraventricular thalamic neurons to the bed nucleus of the stria terminalis contribute to regulating states of consciousness during sevoflurane anesthesia.

(ANESTHESIOLOGY 2022; 136:709–31)

General anesthetics have been widely used in surgery for nearly two centuries because they can induce reversible unconsciousness and maintain physiologic stability. While great progress has been made in our understanding of how general anesthetics work at the molecular level, little is known about how anesthetics cause a loss

Supplemental Digital Content is available for this article. Direct URL citations appear in the printed text and are available in both the HTML and PDF versions of this article. Links to the digital files are provided in the HTML text of this article on the Journal's Web site (www.anesthesiology.org). This article has a visual abstract available in the online version.

Submitted for publication May 12, 2021. Accepted for publication January 21, 2022. Published online first on March 9, 2022.

Jia-Yan Li, M.D., Ph.D.: Department of Anesthesiology, Tongji Hospital, Tongji Medical College, Huazhong University of Science and Technology, Wuhan, China; and Department of Anesthesiology, First Affiliated Hospital, Sun Yat-sen University, Guangzhou, China.

Shao-Jie Gao, M.M.: Department of Anesthesiology, Tongji Hospital, Tongji Medical College, Huazhong University of Science and Technology, Wuhan, China.

Ran-Ran Li, Ph.D.: Department of Physiology, School of Basic Medicine, Tongji Medical College, Huazhong University of Science and Technology, Wuhan, China.

 Anesthesiology 2022; 136:709–31. DOI: 10.1097/ALN.0000000000004195

<zdoi; 10.1097/ALN.0000000000004195>

of consciousness in neural networks.[1–3] Recent studies have indicated that anesthetic-induced unconsciousness arises via specific interactions with neural circuits that regulate the endogenous sleep–wake systems in the central nervous system,[1,4] such as the parabrachial nucleus,[5] lateral hypothalamus,[6] locus coeruleus,[7,8] tuberomammillary nucleus,[9] ventral tegmental area,[10,11] basal forebrain,[12] ventrolateral preoptic nucleus,[13] and lateral habenula.[14] Multiple sites participate in the maintenance of wakefulness and promote arousal from general anesthesia. However, whether other critical arousal-promoting areas and their neural circuits are implicated in the modulation of consciousness under general anesthesia remains largely unknown.

The paraventricular thalamus, a vital constituent of the midline nucleus of the thalamus, plays a pivotal role in the maintenance of wakefulness.[15] The paraventricular thalamus receives afferent projections from multiple regions involved in the regulation of general anesthesia, including the parabrachial nucleus,[5,16] locus coeruleus,[7,17] dorsal raphe nuclei,[18] hypothalamus,[6,19] and prefrontal cortex,[20] and sends extensive outputs to the limbic system.[21] Recent studies have revealed that the limbic system plays an essential role in anesthetic-induced loss of consciousness.[22] Therefore, we hypothesized that the paraventricular thalamus may be the key hub for the regulation of states of consciousness in general anesthesia. However, the potential mechanism in neural circuits remains unclear.

The bed nucleus of the stria terminalis, located in the limbic forebrain, regulates a variety of endocrine and autonomic nervous responses mainly by projecting to the relay nucleus of the autonomic nervous system, hypothalamus, and central amygdala and plays an important role in stress, fear, and anxiety.[23] The activation of γ-aminobutyric acid–mediated (GABAergic) neurons in the bed nucleus of the stria terminalis promotes the rapid transition from non–rapid eye movement sleep to an awake state in mice.[24] Recent studies have shown that calretinin-positive neurons in the paraventricular thalamus project directly to the bed nucleus of the stria terminalis, and this pathway mediates starvation-induced arousal behavior.[25] Therefore, we speculate that the glutamatergic neurons of the paraventricular thalamus also project to the bed nucleus of the stria terminalis and play a role in modulating the states of consciousness in sevoflurane anesthesia.

To test this hypothesis, we first investigated c-Fos expression in the paraventricular thalamus during sevoflurane anesthesia. We then used anterograde and retrograde tracing strategies to identify the synaptic connections between the paraventricular thalamus and the bed nucleus of the stria terminalis, respectively. Next, we selectively inhibited the paraventricular thalamus bed nucleus of the stria terminalis pathway chemogenetically to explore its role in the time of induction and emergence during sevoflurane anesthesia. Cortical electroencephalogram (EEG) activity was also recorded during the induction and recovery period of sevoflurane anesthesia. We further optogenetically activated paraventricular thalamus glutamatergic neurons or their pathways to observe their effects on the maintenance of light sevoflurane anesthesia under continuous steady-state general anesthesia and deep anesthesia with burst-suppression conditions.

Materials and Methods

Animal Care

In all experiments, male and female C57BL/6J mice and male Vglut2-IRES-Cre and Vgat-IRES-Cre mice weighing 20 to 30 g (8 to 10 weeks old) were used in this study. The male C57BL/6J mice were obtained from Tongji Medical College Experimental Animal Center (Huazhong University of Science and Technology, Wuhan, China; certificate 42009800002519/SCXK(E)2016-0009). The Vglut2-IRES-Cre and Vgat-IRES-Cre mice were obtained from Wuhan National Laboratory for Optoelectronics (Huazhong University of Science and Technology). All mice were housed in a temperature-controlled (22 ± 1°C) and humidity-controlled (50 ± 5%) room with food and water *ad libitum* under an automatically controlled 12 h light/12 h dark cycle (lights on from 7 AM to 7 PM). All procedures involving animals were approved by the Hubei Provincial Animal Care and Use Committee (Wuhan China) and were in accordance with the experimental guidelines of the Animal Experimentation Ethics Committee of Tongji Hospital, Huazhong University of Science and Technology. In this study, we applied online randomization tools (https://www.random.org/lists/) to assign animals to each group, and the animals were tested in sequential order. The experimenters conducting all behavior tests were blinded to group allocation.

Wei Wang, Ph.D.: Department of Physiology, School of Basic Medicine, Tongji Medical College, Huazhong University of Science and Technology, Wuhan, China.

Jia Sun, M.M.: Department of Anesthesiology, Tongji Hospital, Tongji Medical College, Huazhong University of Science and Technology, Wuhan, China.

Long-Qing Zhang, M.M.: Department of Anesthesiology, Tongji Hospital, Tongji Medical College, Huazhong University of Science and Technology, Wuhan, China.

Jia-Yi Wu, M.M.: Department of Anesthesiology, Tongji Hospital, Tongji Medical College, Huazhong University of Science and Technology, Wuhan, China.

Dai-Qiang Liu, M.D., Ph.D.: Department of Anesthesiology, Tongji Hospital, Tongji Medical College, Huazhong University of Science and Technology, Wuhan, China.

Pei Zhang, Ph.D.: Department of Neurobiology, School of Basic Medicine, Tongji Medical College, Huazhong University of Science and Technology, Wuhan, China.

Bo Tian, M.D., Ph.D.: Department of Neurobiology, School of Basic Medicine, Tongji Medical College, Huazhong University of Science and Technology, Wuhan, China.

Wei Mei, M.D., Ph.D.: Department of Anesthesiology, Tongji Hospital, Tongji Medical College, Huazhong University of Science and Technology, Wuhan, China.

Virus Injection

The mice were anesthetized with sodium pentobarbital (50 mg/kg, intraperitoneally) and fixed in a stereotaxic apparatus (RWD Life Science Co. Ltd., China). The eyes were covered with ophthalmic ointment. The body temperature of the anesthetized animals was monitored and maintained at 35 to 37°C by a far-infrared warming pad (RightTemp, Kent Scientific, USA). The heart rate and oxygen saturation were monitored by a MouseSTAT clip sensor (MouseSTAT, Kent Scientific, USA) during surgery. Additional subcutaneous bupivacaine for analgesia was applied to expose the skull, and virus was injected using a glass pipette (opening, 15 to 20 μm) with a stereotaxic injector from Stoelting (USA) as previously described.[26] After injection, the syringe was left in place for 10 min to allow the diffusion of the virus and then slowly retracted. For EEG recordings, 3 weeks after virus injection, the mice were implanted with extradural EEG electrodes for EEG recordings. Briefly, two stainless steel screws were placed in the prefrontal cortex (anterior-posterior, 1.75 mm anterior to bregma; medio-lateral, 0.4 mm lateral to bregma) and cerebellum. Electrodes were then secured to the skull using dental adhesive resin cement (C&B-Superbond; Parkell Inc., USA).

For anterograde tracing, AAV-Ef1α-DIO-ChR2-mCherry (AAV2/9, 4.33E+13 vg/ml, 200 nl; Obio Technology Co. Ltd., China) was injected into the paraventricular thalamus of vglut2-Cre mice. After 4 weeks, the mice were perfused with 4% paraformaldehyde, and the projections from paraventricular thalamus glutamatergic neurons to other brain regions were explored by imaging whole-brain sections using an automatic scanning fluorescence microscope (SV120, Olympus, Japan).

For retrograde monosynaptic tracing, Cre-dependent helper viruses, including AAV-EF1α-DIO-TVA-green fluorescent protein (AAV2/9, 2.0E+12 vg/ml) and AAV-EF1α-DIO-RVG (AAV2/9, 2.0E+12 vg/ml, 1:1, 100 nl), were injected into the bed nucleus of the stria terminalis (anterior-posterior,: +0.26 mm; medio-lateral: −1.0 mm; dorsal-ventral: −4.05 mm) of vglut2-Cre mice or vgat-Cre mice, respectively. After 3 weeks, rabies virus (RV-ENVA-ΔG-dsRed, 2.0E+08 infectious units/ml, 200 nl) was microinjected into the same site of the bed nucleus of the stria terminalis.

Anesthesia Behavioral Experiments

We produced an open-circuit anesthetizing apparatus that ensured identical gaseous anesthetic delivery to each of eight mice in isolated transparent cylindrical chambers while maintaining a constant 37°C environment. The mice were placed in a cylinder with 100% oxygen for habituation for 2 h for 3 consecutive days before testing. The time to the loss of the righting reflex was measured after 1 l/min 100% oxygen with 2.4% sevoflurane was administered, the chambers were rotated 180° every 15 s, and the time to the loss of the righting reflex (induction time) was considered as the time when mice first lost their righting reflex for more than 30 s from the time of sevoflurane initiation. After a 30-min exposure to 2.4% sevoflurane, the sevoflurane was shut off, and the time to the recovery of the righting reflex (emergence time) was defined as the interval from the termination of anesthetic inhalation to the return of the righting reflex. The concentration of sevoflurane was monitored by an anesthetic agent analyzer (G60, Philips, China).

To assess sevoflurane responsiveness with a higher precision, the concentration at which 50% of the mice lost their righting reflex and the concentration at which 50% of the mice recovered their righting reflex were measured as described previously.[27] The EC_{50} was calculated from the dose–response equation. To determine the concentration at which 50% of the mice lost their righting reflex, the initial concentration of sevoflurane was set at 0.7 vol%, and the concentrations were increased by 0.2 vol% every 15 min. The chambers were rotated 180° during the last 2 min of this period to observe whether the righting reflex of the mice had disappeared, and the number of animals that lost their righting reflex at each concentration was recorded. The experiments ended when all animals had lost their righting reflex. To determine the concentration at which 50% of the mice recovered their righting reflex, all of the mice were anesthetized with 2.1% sevoflurane for 30 min, and the concentration was decreased in decrements of 0.2% until all of the mice had recovered their righting reflex. The number of mice that had recovered their righting reflex at each concentration was counted. The concentration of sevoflurane was monitored by an anesthetic agent analyzer (G60, Philips, China). The chamber temperature was maintained at 37°C using a heating pad during the whole experiment.

Arousal Scoring

Arousal behaviors were scored as described previously.[10,28] Briefly, spontaneous actions of the limbs, head, and tail were rated on a scoring sheet with three levels, including absent, mild, or moderate in intensity, and were scored 0, 1, or 2, respectively. In addition, if the loss of the righting reflex remained in the mouse, righting was scored as 0, and if all four paws of the mouse touched the ground, righting was scored as 2. Walking was also scored with three levels as follows: made no further movements (0), crawled without raising the abdomen off the floor (1), and walked with all four paws with the abdomen off the floor (2). The total score for each mouse was determined by the sum of all categories.

Whole-cell Recordings

Whole-cell recordings were conducted as described previously.[29] Briefly, after 4 weeks of viral expression, the mouse brain was rapidly removed from the skull and submerged in ice-cold oxygenated slice-cutting solution containing 125 mM NaCl, 3.5 mM KCl, 25 mM $NaHCO_3$, 1.25 mM

NaH_2PO_4, 0.1 mM $CaCl_2$, 3 mM $MgCl_2$, and 10 mM glucose. Acute coronal brain slices containing the paraventricular thalamus were cut at 200- or 400-μm thickness with a vibratome (VT1000S, Leica, Germany). For neuronal whole-cell recording, the slices were kept at 32°C for 1 h after cutting, kept at subsequently at room temperature before use, and then maintained in ice-cold artificial cerebrospinal fluid containing 125 mM NaCl, 25 mM $NaHCO_3$, 1.25 mM NaH_2PO_4, 3.5 mM KCl, 2 mM $CaCl_2$, 1 mM $MgCl_2$, and 10 mM glucose (saturated with 95% O_2 and 5% CO_2). Neurons in the paraventricular thalamus expressing mCherry were clamped with borosilicate glass micropipettes (4 to 7 MΩ). The pipette intracellular solution contained 140 mM potassium gluconate, 13.4 mM sodium gluconate, 0.5 mM $CaCl_2$, 1.0 mM $MgCl_2$, 5 mM EGTA, 10 mM HEPES, 3 mM Mg^{2+}–adenosine triphosphate, and 0.3 mM Na^+-guanosine triphosphate; 280 to 290 mOsm/l (pH 7.4; osmolarity, 280 to 290 mOsm/kg). The data were obtained using a MultiClamp 700B amplifier and pClamp 10 software (Molecular Devices, USA), digitized at 2 to 10 kHz, and filtered at 2 kHz. The patch-clamp recording data were analyzed by Clampfit 9.0 (Molecular Devices).

To verify the functional validity of AAV-hM4D(Gi), after baseline data were recorded for 5 min, clozapine *N*-oxide was applied to the bath for 2 min, and the cells were inhibited using clozapine *N*-oxide (10 μM). To verify the function of AAV-ChR2, mCherry-expressing neurons were stimulated by blue light (473 nm, 10 Hz, a duration of 10 ms) through an optical fiber placed above the cell.

EEG Recording and Analysis

EEG signals were amplified using a Microelectrode AC amplifier model 1700 (A-M Systems, USA) and digitized at a sampling rate of 500 Hz using a PCIe 6323 data acquisition board (National Instruments, USA), and EEG signals were recorded using Spikehound software (Neurobiological Instrumentation Engineer, USA). The raw EEG signals were analyzed using multitaper methods from the Chronux toolbox (version 2.1.2, http://chronux.org/) in MATLAB 2016a (MathWorks, United Kingdom). EEG power spectra were analyzed as described in previous studies.[30] Briefly, raw EEG data were band-pass filtered (1 to 80 Hz) and band-block filtered (48 to 52 Hz) to remove line noise and were computed for a window size of 4 s (50% overlapping) within the frequency range of 0.5 to 50 Hz using a 5-taper in fast Fourier transform. The average power spectral density and the normalized power spectral density were calculated for the delta (0.5 to 4 Hz), theta (4 to 8 Hz), alpha (8 to 15 Hz), beta (15 to 25 Hz), and gamma (25 to 50 Hz) bands. The normalized power spectral density was performed on the data from the period of induction (5 min after the initiation of anesthesia) and emergence (5 min after the discontinuation of the anesthetic), and the average power spectral density was determined during the optogenetic stimulation period (120 s before and after blue light stimulation during the 2.5% sevoflurane anesthesia-induced burst-suppression period).

The burst-suppression ratio was used to quantify the state of burst suppression and calculated as described previously.[31] Briefly, the original EEG data were first band-pass filtered (10 to 80 Hz) and band-block filtered (48 to 52 Hz) and then detrended and smoothed by convolution with a Gaussian function. Next, EEG bursts were preliminarily assigned a value of 0, and EEG suppressions were assigned a value of 1 to produce a binary time series. Finally, this binary time series was smoothed to calculate the burst-suppression ratio over time with a window function. EEG suppression events were defined based on their voltage (amplitude within −15 to 15 μV) and duration (minimal duration, 200 ms or less), and the events were also regarded as the same suppression when the interevent interval was less than 50 ms. EEG epochs between suppression periods were viewed as EEG burst events.

In Vivo Chemogenetic Manipulation

To inhibit paraventricular thalamus glutamatergic neurons, C57BL/6J mice were injected with AAV-CaMKIIa-hM4D(Gi)-mCherry (AAV2/9, 1.18E + 13 vg/ml, 200 nl; Obio Technology Co. Ltd., China) or AAV-CaMKIIa-mCherry (AAV2/9, 1.08E + 13 vg/ml 200 nl; Obio Technology Co. Ltd.) as a control. To inhibit the paraventricular thalamus bed nucleus of the stria terminalis pathway, AAV_{retro}-hSyn-Cre (AAV2/retro, 2.0E+12 vg/ml; BrainVTA Co. Ltd., China) was bilaterally injected into the bed nucleus of the stria terminalis, and then AAV-EF1α-DIO-hM4D(Gi)-mCherry (AAV2/9, 2.0E+12 vg/ml; BrainVTA Co. Ltd.) or AAV-EF1α-DIO-mCherry (AAV2/9, 2.0E+12 vg/ml; BrainVTA Co. Ltd.) was injected into the paraventricular thalamus of C57BL/6J mice. For chemogenetic experiments, 3 weeks after virus injection, 3 mg/kg clozapine *N*-oxide (Sigma, USA) or saline was administered intraperitoneally 1 h before all behavior testing.

In Vivo Optogenetic Manipulation

For optogenetic activation of paraventricular thalamus glutamatergic neurons, AAV-CaMKIIa-ChR2-mCherry-WPREs (AAV2/9, 2.0E + 12 vg/ml, 200 nl; BrainVTA Co. Ltd., China) or AAV-CaMKIIa-mCherry-WPREs (AAV2/9, 2.0E+12 vg/ml, 200 nl; BrainVTA Co. Ltd.) were delivered into the paraventricular thalamus (anterior-posterior = –1.00 mm; medio-lateral = +0.55 mm; dorsal-ventral = –2.95 mm, with a 10-degree angle to the midline), and an optical fiber was implanted above the paraventricular thalamus (anterior-posterior = –1.00 mm; medio-lateral = +0.55 mm; dorsal-ventral = –2.85 mm, with a 10-degree angle to the midline). To optogenetically activate the paraventricular thalamus bed nucleus of the stria terminalis pathway, AAV-EF1α-DIO-ChR2-mCherry (AAV2/9, 4.33E+12

vg/ml, 200 nl; Obio Technology Co. Ltd., China) or AAV-EF1α-DIO-mCherry (control) was injected into the paraventricular thalamus of vglut2-Cre mice, and the optical fiber cable was implanted into the bed nucleus of the stria terminalis (anterior-posterior = +0.26 mm; medio-lateral = –1.0 mm; dorsal-ventral = –3.95 mm) and then fixed to the skull using dental cement. The mice were connected *via* an optical fiber cannula to a laser diode (Newton Inc., China). To stimulate paraventricular thalamus glutamatergic neurons or the paraventricular thalamus bed nucleus of the stria terminalis pathway, optogenetic manipulation (laser of 473 nm, 10-ms pulses at 10 Hz for 120 s) was conducted during all behavior testing as described previously.[15] Light intensities at the tip of the optical fiber cannula were tested by a power meter (PM100D, Thorlabs, Germany) before the experiment and calibrated to emit 10 to 15 mW/mm^2.

For anesthesia behavior testing, the mice were optically stimulated at the initiation of sevoflurane exposure until they lost their righting reflex during induction. During emergence, optical stimulation was delivered from the time sevoflurane administration stopped until the animals recovered their righting reflex. For optogenetic manipulation during sevoflurane anesthesia maintenance, the animals were initially administered 2.5% sevoflurane for 20 min and then placed in a supine position. Then the sevoflurane concentration was reduced to 1.4%. If the animals showed any signs of the recovery of their righting reflex, the concentration was increased by 0.1% until the loss of the righting reflex was maintained at a constant concentration for at least 20 min. In our experiments, sevoflurane concentrations ranging from 1.4 to 1.5% were used to maintain light sevoflurane anesthesia. Optogenetic manipulation was performed for 2 min during continuous, steady-state general anesthesia with sevoflurane to score arousal behavior. In addition, 2.5% sevoflurane was delivered for 30 min to induce a stable burst-suppression pattern, and optogenetic stimulation was performed for 2 min under burst-suppression conditions.

Histology

For c-Fos immunofluorescence staining, the mice were administered 2.4% (1 minimum alveolar concentration) sevoflurane inhalation for 2 h. After sevoflurane anesthesia, the mice were killed immediately and perfused with 0.01 M phosphate-buffered saline followed by 4% paraformaldehyde. After perfusion, the brains were removed and stored in 4% paraformaldehyde overnight at 4°C for postfixation and dehydrated in 30% sucrose at 4°C until they sank. The brains were then serially sectioned on a freezing microtome (CM1900, Leica, Germany) at –20°C. For c-Fos or vglut2 immunofluorescence staining, briefly, the membrane permeability of sections was strengthened with 0.3% Triton X-100/phosphate-buffered saline for 15 min, and the sections were blocked with 10% goat serum in phosphate-buffered saline for 1 h and incubated overnight at 4°C with rabbit anti-c-Fos antibody (1:250; Abcam, United Kingdom) or anti-vglut2 antibody (1:200; Abcam, United Kingdom). After rinsing with phosphate-buffered saline, the sections were incubated with anti-rabbit secondary antibodies coupled to DyLight-488 (1:300; Alexa Fluor, Molecular Probes Inc., USA) for 2 h at room temperature. After another three 10-min washes with phosphate-buffered saline, the slides were covered with DAPI (AR1177, Boster, China) for 5 min, and the sections were washed, mounted, and coverslipped. Images were captured on a fluorescence microscope (DM2500, Leica Microsystems, Germany). The experimenters involved in microscopy analysis were blinded to group allocation. The mean fluorescence intensity of c-Fos–positive neurons was analyzed on alternate sections in the paraventricular thalamus (approximately from bregma –1.06 to –2.06 mm; n = 6, where n refers to the number of animals, three sections per mouse). In response to peer review, additional experiments for the change in c-Fos expression in the paraventricular thalamus in female mice during sevoflurane anesthesia were added.

Statistical Analysis

In this study, we injected virus into the paraventricular thalamus in 135 male mice. Histological tests were carried out after the behavior tests to identify the position of virus infection. Forty-seven mice with inaccurate injection sites, inaccurate placement of optic fibers, or poor recovery after virus injection were excluded, and the other 88 mice were included in the data analysis. The paraventricular thalamus bed nucleus of the stria terminalis pathway was manipulated in 112 male mice. Eighty-nine mice were used for data analysis, and 23 mice with inaccurate injection sites or poor conditions were excluded. In this study, n refers to the number of animals. In response to peer review, the paraventricular thalamus was manipulated in an additional 60 female mice; 12 mice with inaccurate injection sites were excluded, and the other 48 mice were included in the data analysis. No *a priori* statistical power calculation was performed. Sample sizes were chosen based on similar experiments using chemogenetic and optogenetic methods. Before analysis, all data were tested by the Shapiro–Wilk normality test. Parametric tests or nonparametric tests were used according to the results of the normality tests. Group differences in cell counts were tested with unpaired Student's *t* tests. To determine the EC_{50} at the loss of the righting reflex or the recovery of the righting reflex and the corresponding 95% CI, the population percentage of loss/recovery of the righting *versus* the log scale of inhaled anesthetic concentration curve was generated by nonlinear regression with a variable slope (multiple parameters) using GraphPad Prism 6.0 (GraphPad Software, USA). A Bayesian Monte Carlo method was applied to evaluate the efficacy of optical stimulation for the restoration of righting during continuous, steady-state general anesthesia with sevoflurane, as previously described.[10,28] For this calculation, we assumed a binomial model as the sampling density or likelihood

function for the tendency of mice in a given group to have the righting response. We considered the uniform density in the interval (0,1) as the prior density of each group since it is noninformative. The posterior density of each group is the beta density because the prior density is proportional to the likelihood function of the binomial model, and this uniform density was regarded as the conjugate prior density for the beta density. We calculated the posterior probability that the propensity to right of one group was greater than that of the other group. The posterior probability of the difference in the propensity to right between the two groups (ChR2-on and mCherry-on) was obtained from beta distributions. The Bayesian CIs that did not include 0 and a posterior probability greater than 0.95 were considered statistically significant. The Bayesian estimation was conducted and analyzed by applying appropriate codes in MATLAB 2016a (MathWorks, United Kingdom). Arousal scoring was tested using a Mann–Whitney U test on the total score. Differences in the burst-suppression ratio and the average power spectral density before and during optical stimulation were analyzed using paired Student's *t* tests. Behavior testing, data were analyzed by ordinary one-way ANOVA followed by a *post hoc* Bonferroni test. EEG-normalized power spectral density changes during the induction or emergence period were analyzed by two-way repeated-measures ANOVA followed by a *post hoc* Bonferroni test. The data are expressed as the mean ± SD or median ± interquartile range (25th, 75th). In all cases, a value of $P < 0.05$ was considered statistically significant.

Results

Sevoflurane Inhibits Neuronal Activity in the Paraventricular Thalamus

To determine whether sevoflurane anesthesia is associated with neuron activities in the paraventricular thalamus, we explored the changes in neuronal activities in the paraventricular thalamus under sevoflurane anesthesia. In response to peer review, we examined the expression of c-Fos, a marker of neuronal activity, after treatment with 2.4% (1 minimum alveolar concentration) sevoflurane inhalation for 2 h in both male and female mice. We found that neuronal activities in the paraventricular thalamus were suppressed in both male and female mice under sevoflurane anesthesia, suggesting that neuronal activities in the paraventricular thalamus can be regulated by sevoflurane anesthesia (fig. 1, A and B; Supplemental Digital Content 1, fig. S1, A and B [http://links.lww.com/ALN/C836]).

Effects of Paraventricular Thalamus Glutamatergic Neuron Inhibition on Sevoflurane Induction, Emergence Time, and Anesthesia Sensitivity

To selectively manipulate paraventricular thalamus glutamatergic neurons, an adeno-associated virus expressing engineered hM4D(Gi) receptor (AAV-CaMKIIa-hM4D(Gi)-mCherry) or a control virus (AAV-CaMKIIa-mCherry) was microinjected into the paraventricular thalamus (fig. 2A). Extensive mCherry fluorescence was detected in the paraventricular thalamus at 3 weeks after microinjection (fig. 2B). By obtaining whole-cell recordings from acute brain slices (fig. 2C), we further confirmed that the application of clozapine *N*-oxide (10 μM) could significantly inhibit paraventricular thalamus glutamatergic neurons, suggesting that the activity of hM4D(Gi)-expressing paraventricular thalamus glutamatergic neurons could be suppressed by clozapine *N*-oxide *in vitro*.

The loss of the righting reflex and the recovery of the righting reflex in mice have been considered surrogates of anesthetic-induced loss and recovery of consciousness in humans.[32] To further explore the effects of paraventricular thalamus glutamatergic neuron inhibition on sevoflurane-induced loss and recovery of consciousness, the mice were exposed to 2.4% sevoflurane, and the time to the loss of the righting reflex was investigated in male mice. In response to peer review, female mice were added to this experiment. In addition, we found that the induction time was reduced in the hM4D–clozapine *N*-oxide group compared with that in the hM4D-saline group (male and female: 101 ± 32 *vs.* 132 ± 30 s, $P = 0.009$, n = 24; fig. 2D; male: 116 ± 36 *vs.* 154 ± 23 s, $P = 0.012$, n = 12; Supplemental Digital Content 1, fig. S2A [http://links.lww.com/ALN/C836]; female: 86 ± 20 *vs.* 109 ± 15 s, $P = 0.025$, n = 12; Supplemental Digital Content 1, fig. S3A [http://links.lww.com/ALN/C836]) and the mCherry–clozapine *N*-oxide group (male and female: 101 ± 32 *vs.* 136 ± 34 s, $P = 0.002$, n = 24; fig. 2D; male: 116 ± 36 *vs.* 163 ± 22 s, $P = 0.001$, n = 12; Supplemental Digital Content 1, fig. S2A [http://links.lww.com/ALN/C836]; female: 86 ± 20 *vs.* 110 ± 18 s, $P = 0.019$, n = 12; Supplemental Digital Content 1, fig. S3A [http://links.lww.com/ALN/C836]). After a 30-min 2.4% sevoflurane exposure, the sevoflurane was shut off, and the hM4D group with the delivery of clozapine *N*-oxide showed a significant increase in the duration to the recovery of the righting reflex compared to that in the hM4D-saline group (male and female: 281 ± 88 *vs.* 156 ± 40 s, $P < 0.001$, n = 24; fig. 2E; male: 267 ± 84 *vs.* 157 ± 41 s, $P < 0.001$, n = 12; Supplemental Digital Content 1, fig. S2B [http://links.lww.com/ALN/C836]; female: 295 ± 92 vs. 154 ± 42 s, $P < 0.001$, n = 12; Supplemental Digital Content 1, fig. S3B [http://links.lww.com/ALN/C836]) and the mCherry–clozapine *N*-oxide group (male and female: 281 ± 88 *vs.* 172 ± 48 s, $P < 0.001$, n = 24; fig. 2E; male: 267 ± 84 *vs.* 169 ± 45 s, $P < 0.001$, n = 12; Supplemental Digital Content 1, fig. S2B [http://links.lww.com/ALN/C836]; female: 295 ± 92 *vs.* 176 ± 53 s, $P < 0.001$, n = 12; Supplemental Digital Content 1, fig. S3B [http://links.lww.com/ALN/C836]), indicating that the inhibition of paraventricular thalamus glutamatergic neurons prolonged the sevoflurane anesthesia emergence time.

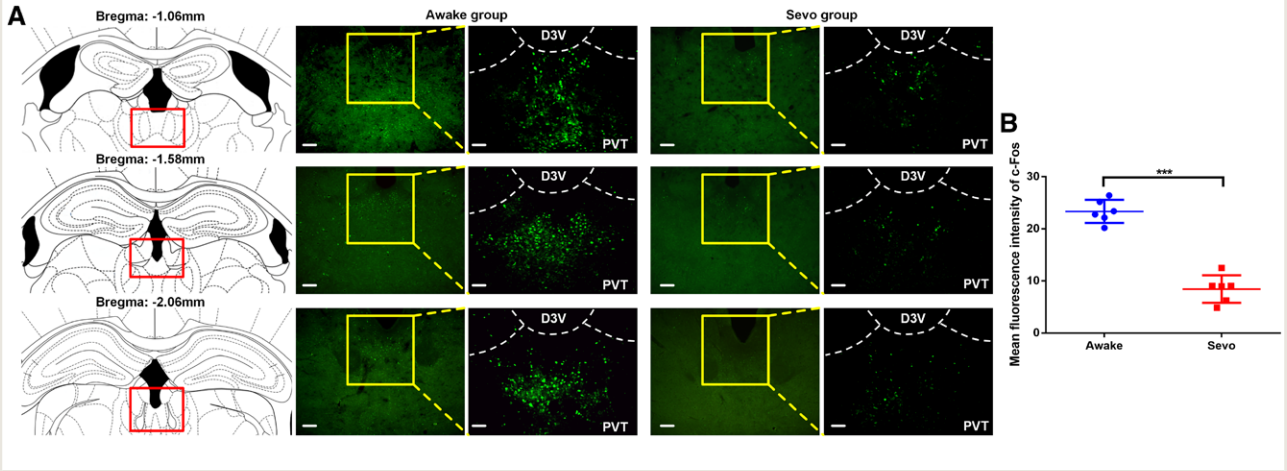

Fig. 1. c-Fos expression in the paraventricular thalamus under sevoflurane anesthesia. (*A*) Representative images of c-Fos immunofluorescence in the paraventricular thalamus between the awake and sevoflurane anesthesia groups in male mice. (*Left*) Representative brain sections stained with c-Fos (*green*). *Scale bars*, 200 μm. (*Right*) Magnified images. *Scale bars*, 100 μm. (*B*) Quantitative analysis of the intensity of c-Fos staining in the paraventricular thalamus. The data are shown as the mean ± SD. ***$P < 0.001$ (n = 6 for each group). D3V, dorsal 3rd ventricle; PVT, paraventricular thalamus; Sevo, sevoflurane.

To further determine the role of paraventricular thalamus glutamatergic neurons in sevoflurane anesthesia sensitivity, the dose–response curve of the percentage of loss of the righting reflex or the recovery of the righting reflex *versus* sevoflurane concentration was plotted. We found that the dose–response curves of both the loss and the recovery of the righting reflex were left-shifted for the hM4D–clozapine *N*-oxide group compared with those in the hM4D-saline group and the mCherry–clozapine *N*-oxide group in male mice. In response to peer review, additional experiments in female mice were added in this experiment. The concentration at which 50% of the mice lost their righting reflex of sevoflurane was significantly decreased in the hM4D–clozapine *N*-oxide group compared with that in the hM4D-saline group (male and female: mean [95% CI], 1.16 [1.12 to 1.20] *vs.* 1.43 [1.40 to 1.46] vol%, $P < 0.001$, n = 20; fig. 2F; Supplemental Digital Content 1, table S1 [http://links.lww.com/ALN/C836]; male: 1.20 [1.18 to 1.21] *vs.* 1.45 [1.44 to 1.46] vol%, $P < 0.001$, n = 10; Supplemental Digital Content 1, fig. S2C, table S2 [http://links.lww.com/ALN/C836]; female: 1.11 [1.04 to 1.18] *vs.* 1.40 [1.35 to 1.46] vol%, $P < 0.001$, n = 10; Supplemental Digital Content 1, fig. S3C, table S3 [http://links.lww.com/ALN/C836]) and the mCherry–clozapine *N*-oxide group (male and female: 1.16 [1.12 to 1.20] *vs.* 1.49 [1.46 to 1.53] vol%, $P < 0.001$, n = 20; fig. 2F; Supplemental Digital Content 1, table S1 [http://links.lww.com/ALN/C836]; male: 1.20 [1.18 to 1.21] *vs.* 1.50 [1.44 to 1.57] vol%, $P < 0.001$, n = 10; Supplemental Digital Content 1, fig. S2C, table S2 [http://links.lww.com/ALN/C836]; female: 1.11 [1.04 to 1.18] *vs.* 1.48 [1.43 to 1.53] vol%, $P < 0.001$, n = 10; Supplemental Digital Content 1, fig. S3C, table S3 [http://links.lww.com/ALN/C836]), and the concentration at which 50% of the mice recovered their righting reflex (EC_{50}) of sevoflurane was lowered in the hM4D–clozapine *N*-oxide group compared with that in the hM4D-saline group (male and female: mean [95% CI], 0.95 [0.86 to 1.03] *vs.* 1.32 [1.29 to 1.34] vol%, $P < 0.001$, n = 20; fig. 2G; Supplemental Digital Content 1, table S1 [http://links.lww.com/ALN/C836]; male: 1.07 [0.94 to 1.22] *vs.* 1.32 [1.29 to 1.36] vol%, $P = 0.009$, n = 10; Supplemental Digital Content 1, fig. S2D, table S2 [http://links.lww.com/ALN/C836]; female: 0.86 [0.81 to 0.91] *vs.* 1.32 [1.27 to 1.36] vol%, $P < 0.001$, n = 10; Supplemental Digital Content 1, fig. S3D, table S3 [http://links.lww.com/ALN/C836]) and the mCherry–clozapine *N*-oxide group (male and female: mean [95% CI], 0.95 [0.86 to 1.03] *vs.* 1.34 [1.29 to 1.40] vol%, $P < 0.001$, n = 20; fig. 2G; Supplemental Digital Content 1, table S1 [http://links.lww.com/ALN/C836]; male: 1.07 [0.94 to 1.22] *vs.* 1.38 [1.34 to 1.42] vol%, $P = 0.003$, n = 10; Supplemental Digital Content 1, fig. S2D, table S2 [http://links.lww.com/ALN/C836]; female: 0.86 [0.81 to 0.91] *vs.* 1.30 [1.23 to 1.36] vol%, $P < 0.001$, n = 10; Supplemental Digital Content 1, fig. S3D, table S3 [http://links.lww.com/ALN/C836]). Taken together, our results indicate that the blockade of the activities of paraventricular thalamus glutamatergic neurons facilitated induction, delayed emergence, and increased sevoflurane anesthesia sensitivity.

Chemogenetic Inhibition of Paraventricular Thalamus Glutamatergic Neurons Accelerates Cortical Sedation and Suppresses Cortical Arousal from Sevoflurane Anesthesia

To further determine how the inhibition of paraventricular thalamus glutamatergic neurons could affect induction

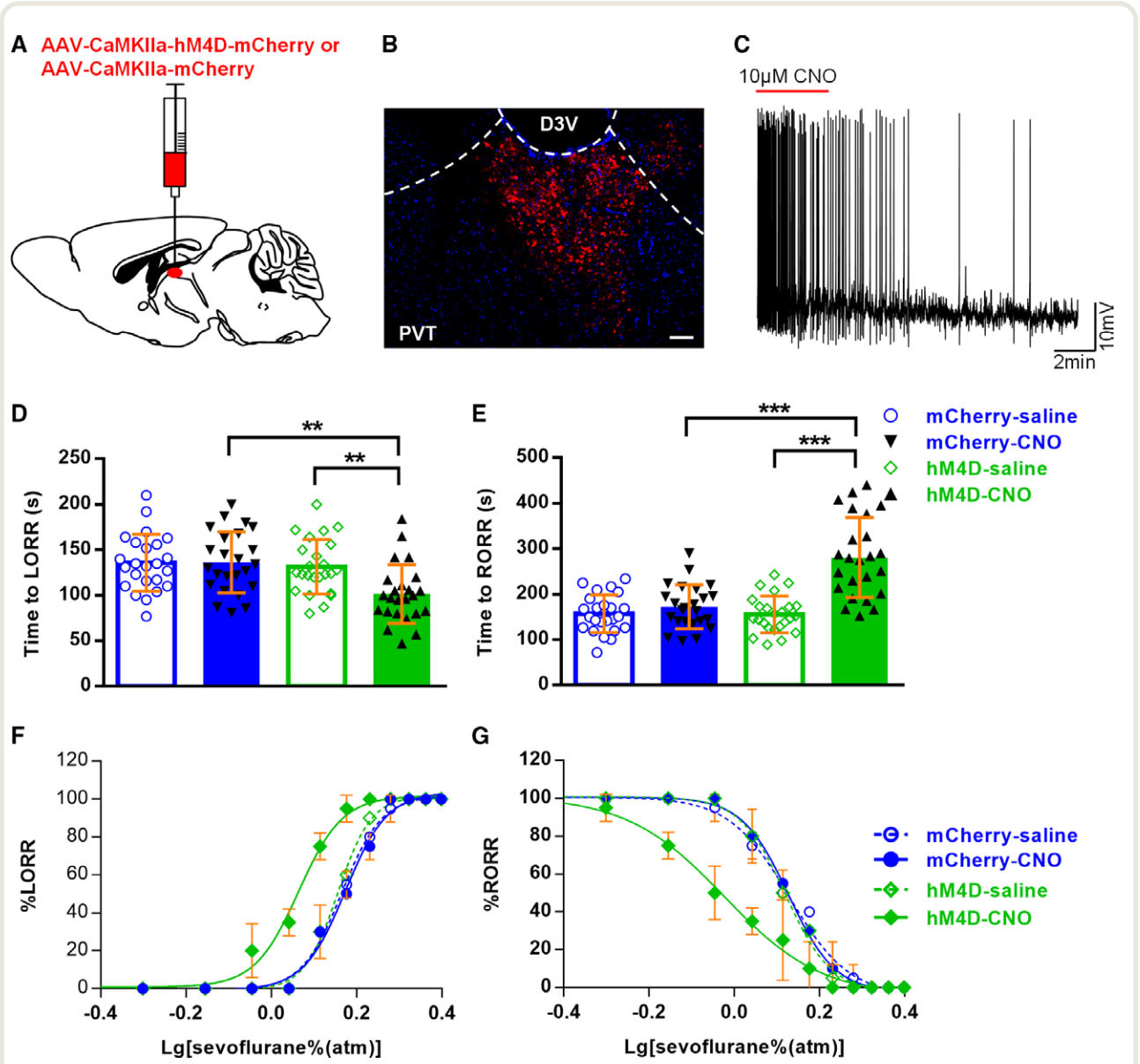

Fig. 2. Effects of chemogenetic inhibition of paraventricular thalamus glutamatergic neurons on sevoflurane induction, emergence time, and anesthesia sensitivity. (*A*) Schematic of virus injection. (*B*) Representative images showing the expression of hM4D(Gi) receptors (*red*) in the paraventricular thalamus. *Scale bar*, 100 μm. (*C*) Whole-cell patch clamping of paraventricular thalamus glutamatergic neurons expressing hM4D showing suppressed action potential responses to the application of clozapine *N*-oxide (10 μM) *in vitro*. (*D* and *E*) Time to induction (*D*) and emergence (*E*) with exposure to 2.4% sevoflurane (1 minimum alveolar concentration) for 30 min after pretreatment with saline or clozapine *N*-oxide in the control group (AAV-CaMKIIa-mCherry) and the hM4D group (AAV-CaMKIIa-hM4D-mCherry), respectively. The data are shown as the mean ± SD (one-way ANOVA). $^{**}P < 0.01$; $^{***}P < 0.001$ (*post hoc* Bonferroni test, hM4D–clozapine *N*-oxide *vs.* hM4D-saline/mCherry–clozapine *N*-oxide, n = 24 for each group). (*F* and *G*) Dose–response curves of the loss of the righting reflex (*F*) and the recovery of the righting reflex (*G*) between paraventricular thalamus inhibition and control mice.

and arousal, we obtained EEG recordings from the somatosensory cortex in male mice. As shown in figure 3, A to C, compared with saline administration, hM4D expression group delivery of clozapine *N*-oxide induced a quick transition from an awake-EEG state to an anesthesia-EEG state because at baseline, the animals were already sedated, with higher delta activity, as described previously.[15] Power spectral density analysis of the EEG signal suggested a prominent interaction between clozapine *N*-oxide and the EEG frequency band during the sevoflurane anesthesia induction and recovery periods. During the anesthesia induction period, the group with the delivery of clozapine *N*-oxide

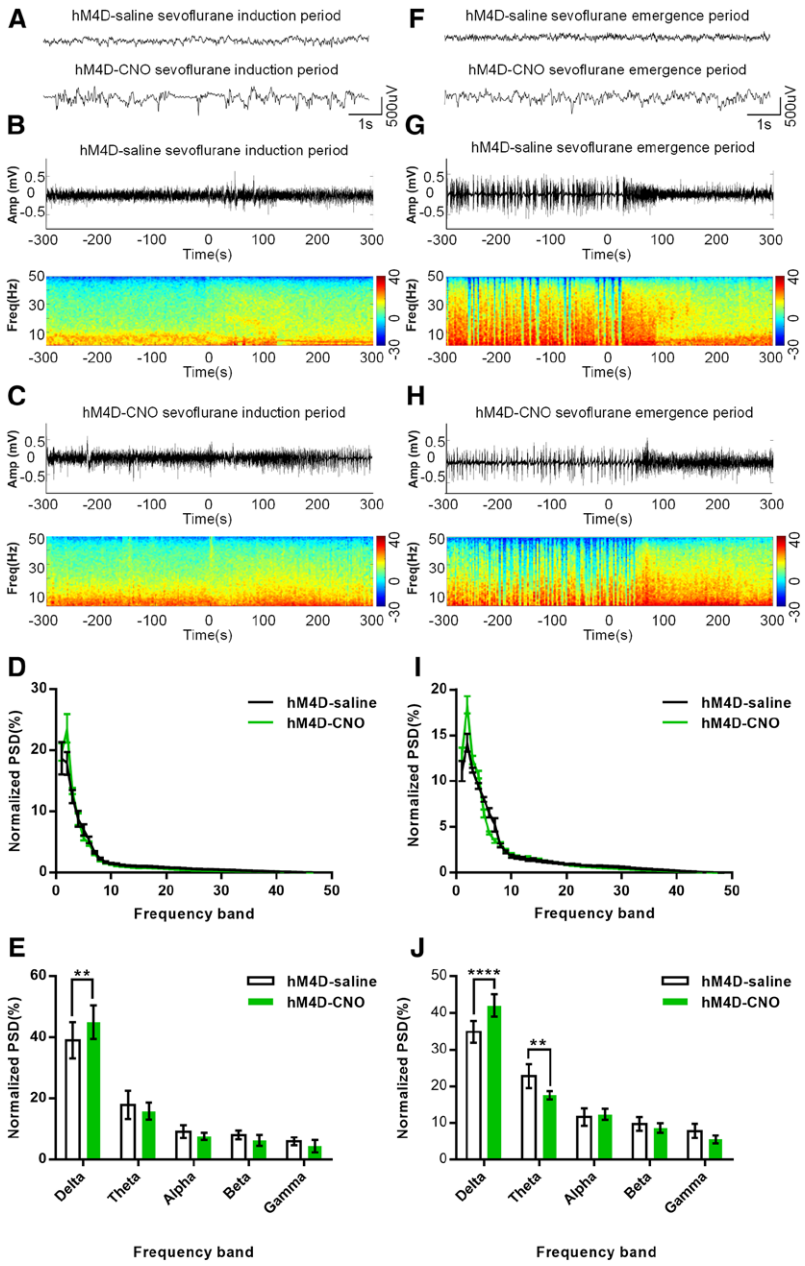

Fig. 3. Chemogenetic inhibition of paraventricular thalamus glutamatergic neurons induced electroencephalogram changes during sevoflurane anesthesia. (*A*) Representative raw electroencephalogram traces during the sevoflurane induction period in hM4D mice after the delivery of clozapine *N*-oxide or saline. (*B* and *C*) Representative electroencephalogram power spectrograms during the induction period after the administration of saline (*B*) or clozapine *N*-oxide (*C*). Time zero on the timeline represents the initiation of sevoflurane anesthesia. (*D*) Electroencephalogram traces 5 min after the initiation of sevoflurane anesthesia were analyzed. Normalized power spectral densities in the hM4D-saline (*black*) and hM4D–clozapine *N*-oxide (*green*) groups during the sevoflurane induction period. (*E*) Quantitative analysis of normalized power spectral density. Compared with the hM4D-saline group, the hM4D–clozapine *N*-oxide group showed a significant increase in electroencephalogram delta power. The data are shown as the mean ± SD (two-way ANOVA). $^{**}P < 0.01$ (*post hoc* Bonferroni test, hM4D–clozapine *N*-oxide *vs.* hM4D-saline, n = 8 for each group). (*F*) Representative raw electroencephalogram traces during the emergence period in hM4D mice after the delivery of clozapine *N*-oxide or saline. (*G* and *H*) Representative electroencephalogram power spectrograms during the sevoflurane anesthesia recovery period in the hM4D-saline (*black*) and hM4D–clozapine *N*-oxide (*green*) groups. Time zero on the timeline indicates the cessation of sevoflurane anesthesia. (*I*) Electroencephalogram traces 5 min after the discontinuation of sevoflurane anesthesia were analyzed. Normalized power spectral density in the hM4D-saline (*black*) and hM4D–clozapine *N*-oxide (*green*) groups during the sevoflurane emergence period. (*J*) In the recovery period, quantitative analysis of normalized power spectral density shows that in the hM4D group, the delivery of clozapine *N*-oxide led to a significant increase in delta power and a decrease in theta power compared with those resulting from the delivery of saline. The data are shown as the mean ± SD (two-way ANOVA). $^{**}P < 0.01$; $^{****}P < 0.0001$ (*post hoc* Bonferroni test, hM4D–clozapine *N*-oxide *vs.* hM4D-saline, n = 8 for each group).

showed a significant increase in the delta band (45.0 ± 5.5%) compared with that in the hM4D-saline group (39.1 ± 6.0%, $P = 0.001$, n = 8), while the other bands (theta, alpha, beta, and gamma bands) showed no significant difference (fig. 3, D and E), indicating that the inhibition of paraventricular thalamus glutamatergic neurons accelerated sevoflurane-induced sedation. During the sevoflurane anesthesia recovery period, the transition from an anesthesia-EEG state to an awake-EEG state was delayed in the hM4D–clozapine *N*-oxide group (fig. 3, F and H). The power in the delta band showed a significant increase in the hM4D–clozapine *N*-oxide group (42.0 ± 3.1%) compared with that in the hM4D-saline group (34.9 ± 3.0%, $P < 0.0001$, n = 8), while the power in the theta band was decreased in the hM4D–clozapine *N*-oxide group (17.6 ± 1.2%) compared with that in the control group (22.8 ± 3.3%, $P = 0.004$, n = 8; fig. 3, I and J). These findings suggest that the inhibition of paraventricular thalamus glutamatergic neurons suppressed cortical arousal from sevoflurane anesthesia.

Optogenetic Activation of Paraventricular Thalamus Glutamatergic Neurons Induces Behavioral Arousal and Reduces the Depth of Anesthesia during the Sevoflurane Anesthesia Maintenance Period

To further test the effects of paraventricular thalamus glutamatergic neurons on sevoflurane anesthesia, we stimulated the neuronal activity of the paraventricular thalamus *in vivo* using optogenetics (fig. 4A). The immunofluorescence results verified that the paraventricular thalamus neurons had been successfully transfected with optogenetic viruses (fig. 4B). Whole-cell recordings showed that neurons expressing the ChR2 virus in the paraventricular thalamus were successfully activated by optical stimulation (fig. 4C). We stimulated the paraventricular thalamus *in vivo* with a 10-ms pulse width of blue light (473 nm) at 10 Hz in male mice according to previous literature.[15] When exposed to 2.4% sevoflurane, constant optogenetic stimulation of the paraventricular thalamus significantly increased the time to the loss of the righting reflex in the ChR2-on group (188 ± 30 s) compared with that in the ChR2-off group (138 ± 33 s, $P = 0.021$, n = 8; fig. 4D) and the mCherry-on group (144 ± 28 s, $P = 0.048$, n = 8; fig. 4D). For sevoflurane anesthesia emergence, the time to recovery of the righting reflex was significantly reduced in the ChR2-on group (102 ± 27 s) compared with that in the ChR2-off group (166 ± 52 s, $P = 0.011$, n = 8; fig. 4E) and the mCherry-on group (159 ± 33 s, $P = 0.029$, n = 8; fig. 4E). These results indicate that the activation of paraventricular thalamus glutamatergic neurons delayed induction and accelerated behavioral arousal from sevoflurane anesthesia.

To further test whether the activation of paraventricular thalamus glutamatergic neurons is capable of restoring states of consciousness during the sevoflurane anesthesia maintenance period, we used optogenetics to instantaneously stimulate neuronal activities in the paraventricular thalamus when mice lost their righting reflex for 20 min during continuous steady-state general anesthesia with 1.4 to 1.5% sevoflurane. We found that optical stimulation of paraventricular thalamus glutamatergic neurons in male mice induced similar evidence of arousal behavior (fig. 4F; Supplemental Digital Content 1, table S5 [http://links.lww.com/ALN/C836]; Supplemental Digital Content 2, video S1 [http://links.lww.com/ALN/C837]), including leg, head, and tail movements (8 of 8), righting (6 of 8), and walking (5 of 8), in mice in the ChR2-on group during the light sevoflurane anesthesia maintenance period (Supplemental Digital Content 1, table S5 [http://links.lww.com/ALN/C836]). To rule out the influence of the light stimulus, we injected AAV-CaMKIIa-mCherry into the paraventricular thalamus as a control experiment, and this evident arousal behavior was scarcely observed in mice in the mCherry-on (Supplemental Digital Content 1, table S5 [http://links.lww.com/ALN/C836]; Supplemental Digital Content 3, video S2 [http://links.lww.com/ALN/C838]) or the ChR2-off group (Supplemental Digital Content 1, table S5 [http://links.lww.com/ALN/C836]). The Bayesian 95% CI for the difference in the propensity of righting derived from the beta distribution between the ChR2-on group and the mCherry-on group was 0.185 to 0.865 under sevoflurane continuous steady-state general anesthesia with optostimulation of paraventricular thalamus glutamatergic neurons at 10 Hz for 120 s (fig. 4, G and H). The posterior probability of the difference in righting between the ChR2-on group and the mCherry-on group greater than 0 was 0.997, which was statistically significant (fig. 4H). These results suggest that the stimulation of paraventricular thalamus glutamatergic neurons was sufficient to evoke behavioral arousal during the light anesthesia maintenance period. In addition, we further explored whether the activation of paraventricular thalamus glutamatergic neurons affects the maintenance period of deep anesthesia under burst suppression. As shown in figure 5, A to E, the photostimulation of the paraventricular thalamus caused a rapid increase in EEG burst duration (fig. 5A) and decreased the burst-suppression ratio from 59.4 ± 19.5 to 11.7 ± 10.4% ($P < 0.001$, n = 7; fig. 5E; Supplemental Digital Content 4, video S3 [http://links.lww.com/ALN/C839]) during the burst-suppression state induced by 2.5% sevoflurane in male mice. Additionally, the average power spectral density analysis of the EEG showed an increase in the delta, alpha, beta, and gamma bands during photostimulation compared with prestimulation (fig. 5, B to D). As shown in figure 5, F to J, there were no significant differences in raw EEG (fig. 5F; Supplemental Digital Content 5, video S4 [http://links.lww.com/ALN/C840]), burst-suppression ratio (fig. 5J), or power spectral densities during optical stimulation compared with prestimulation in mice in the mCherry group (fig. 5, G to I). These results suggest that the stimulation of paraventricular thalamus glutamatergic neurons can drive cortical activation and reduce anesthesia depth during the maintenance period of deep sevoflurane anesthesia.

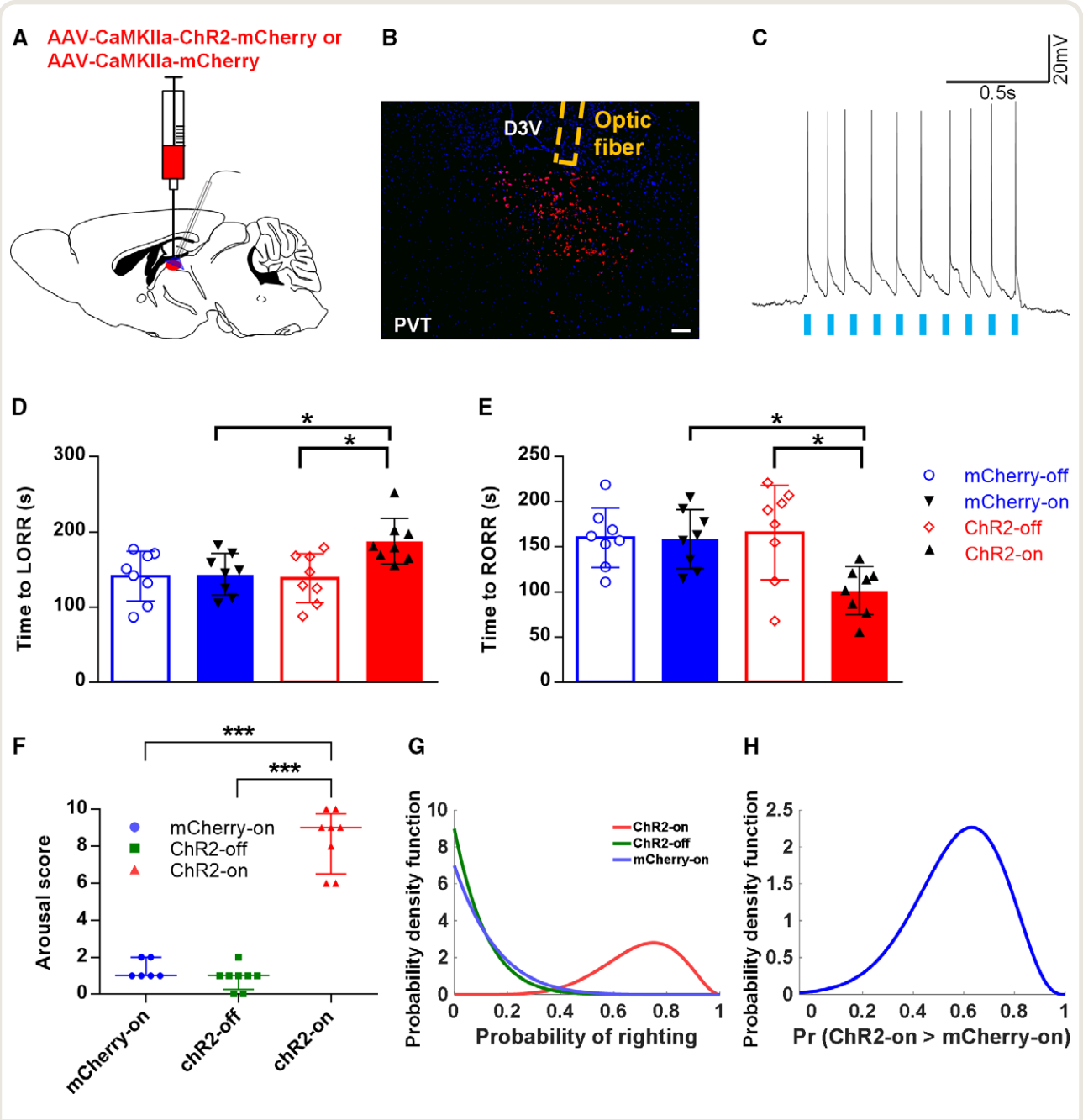

Fig. 4. Optogenetic activation of paraventricular thalamus glutamatergic neurons delayed induction, accelerated emergence, and induced arousal-like responses under continuous steady-state general anesthesia with sevoflurane. (*A*) Schematic representation of virus injection. (*B*) Representative image showing the expression of channelrhodopsin-2 (ChR2) –mCherry (*red*) in the paraventricular thalamus and confirming the location of the optic fiber in the paraventricular thalamus. *Scale bar*, 200 μm. (*C*) Example traces of neuronal firing of ChR2-expressing paraventricular thalamus glutamatergic neurons evoked by 473-nm photostimulation at 10 Hz. (*D* and *E*) Induction time (*D*) and emergence time (*E*) with exposure to 2.4% sevoflurane (1 minimum alveolar concentration) during 10-Hz blue laser stimulation in ChR2-expressing and control mice. The data are shown as the mean ± SD (one-way ANOVA). **P* < 0.05 (*post hoc* Bonferroni test, hM4D–clozapine *N*-oxide *vs.* hM4D-saline/mCherry–clozapine *N*-oxide, n = 8 for each group). (*F*) Total arousal response score for the optical stimulation of paraventricular thalamus glutamatergic neurons (10-ms pulses, 10 Hz, 120 s) during continuous steady-state general anesthesia with 1.4 to 1.5% sevoflurane. The data are shown as the medians and interquartile ranges (25th, 75th). ****P* < 0.001 (n = 8 in the ChR2-on/off group, and n = 6 in the mCherry-on group). (*G*) Posterior densities for the propensity of righting for the ChR2-on (*red*), ChR2-off (*green*), and mCherry-on (*blue*) groups. Posterior densities are obtained from beta distributions. (*H*) Posterior probability of the difference between the ChR2-on group and the mCherry-on group during continuous steady-state general anesthesia with sevoflurane.

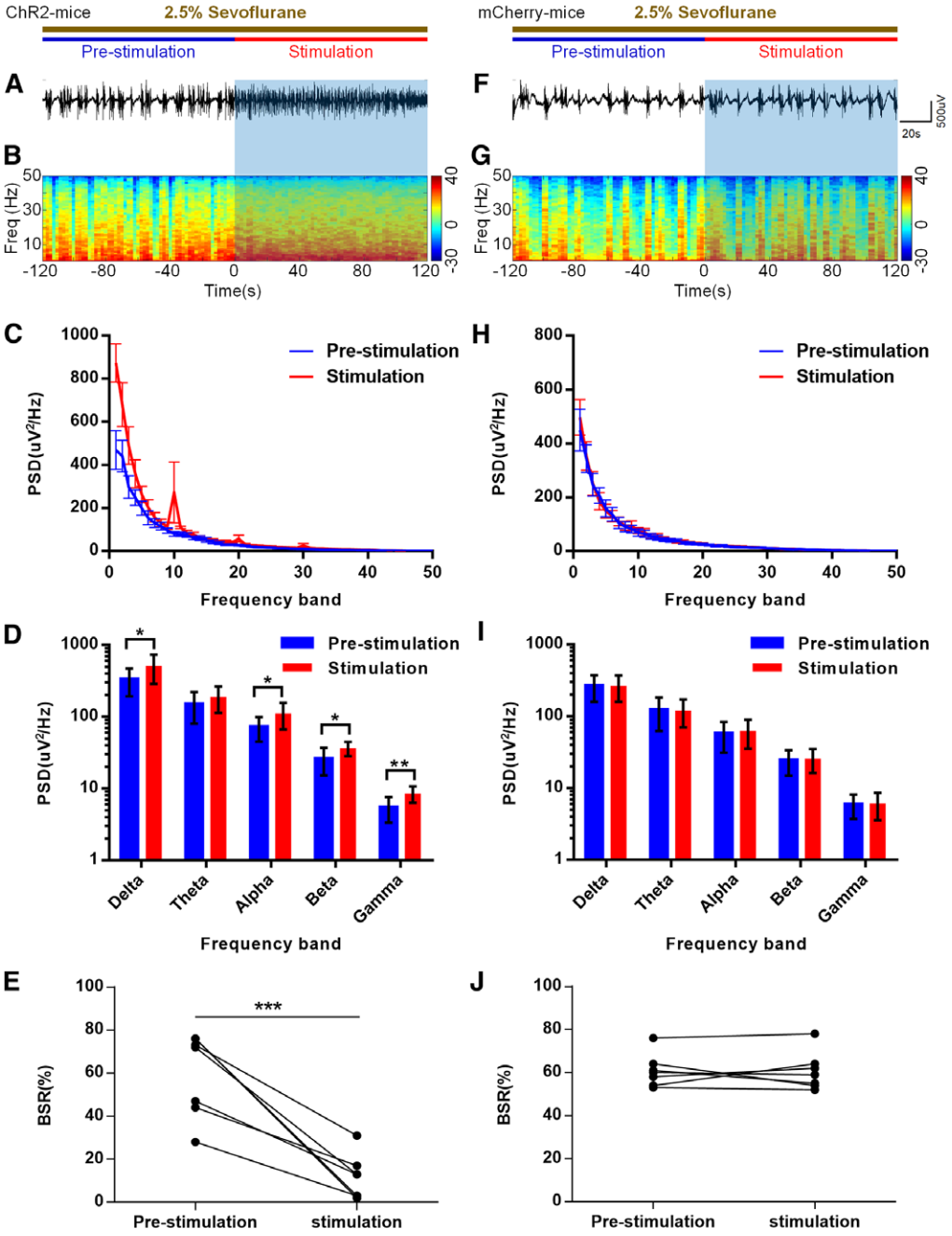

Fig. 5. Optogenetic activation of paraventricular thalamus glutamatergic neurons induced cortical activation under sevoflurane burst-suppression conditions. (*A* and *B*) Representative raw electroencephalogram traces (*A*) and electroencephalogram power spectra (*B*) in a mouse injected with AAV-CaMKIIa-ChR2-mCherry. The *blue shading* represents periods of light stimulation (10-ms pulses; 10 Hz; 120 s). Time zero indicates the beginning of optical stimulation during sevoflurane-induced burst suppression. (*C*) Average power spectral density in the PVT-ChR2 mice computed from 120 s before stimulation (*blue*) to 120 s during optical stimulation (*red*). (*D*) Quantitative analysis of the average power spectral density showed that photostimulation increased the delta, alpha, beta, and gamma power in PVT-ChR2 mice. The data are shown as the mean ± SD). $^{*}P < 0.05$; $^{**}P < 0.01$ (n = 8 in each group). (*E*) The electroencephalogram burst suppression ratio was significantly reduced by optical stimulation during continuous 2.5% sevoflurane anesthesia in PVT-ChR2 mice. $^{***}P < 0.001$ (n = 7 in each group). (*F* and *G*) Typical examples of electroencephalogram traces (*F*) and electroencephalogram power spectra (*G*) in the control group (AAV-CaMKIIa–mCherry). (*H*) Average power spectral density in the control group computed from 120 s before stimulation (*blue*) to 120 s after optical stimulation (*red*). (*I*) Quantitative analysis of the average power spectral density showed no significant difference between the prestimulation and stimulation periods in the control group. (*J*) Effect of optical stimulation on the electroencephalogram burst suppression ratio during continuous sevoflurane anesthesia in the control group ($P = 0.912$, n = 7 for each group).

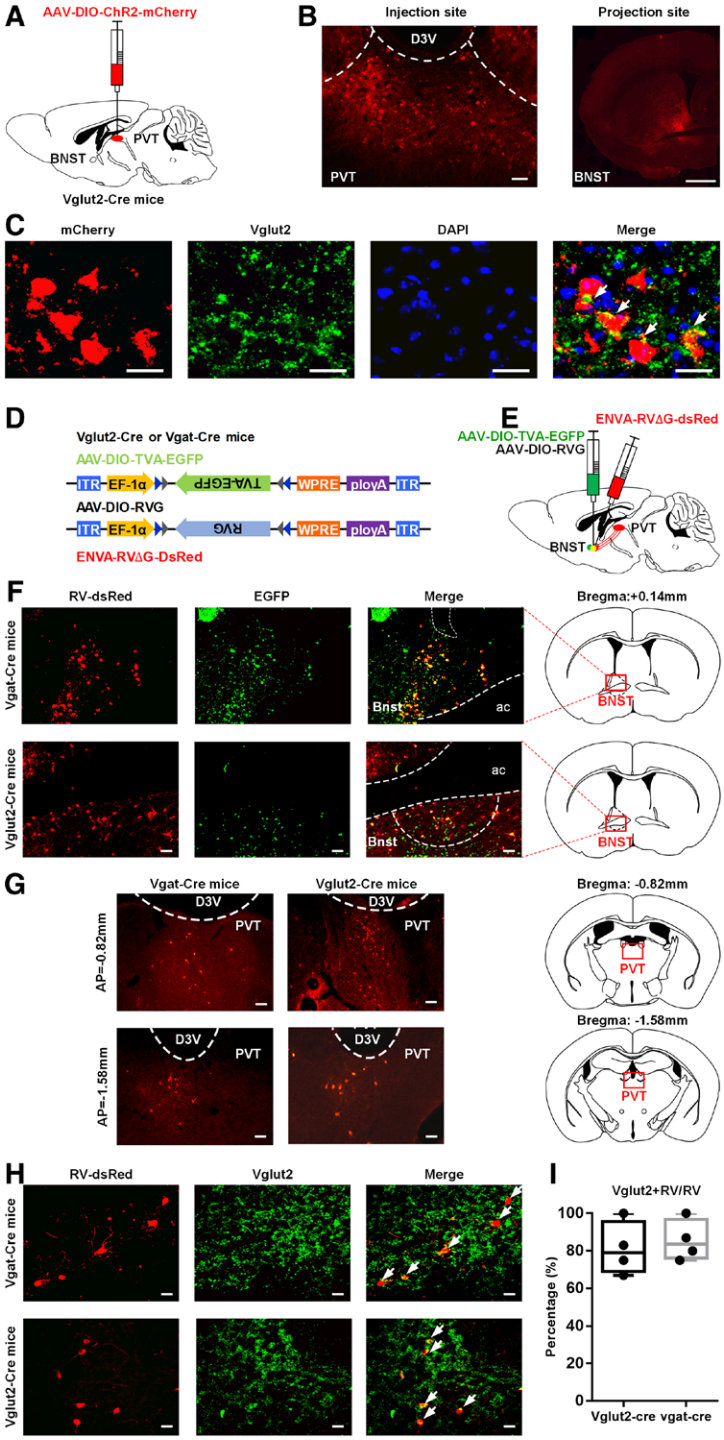

Fig. 6. The paraventricular thalamus glutamatergic neurons project onto the glutamatergic and γ-aminobutyric acid–mediated neurons in the bed nucleus of the stria terminalis. (*A*) Schematic representation of virus injection location and glutamatergic cell type–specific anterograde tracing. (*B*) Representative images showing ChR2-expressing cells in the vglut2$^+$ neurons of the paraventricular thalamus (*left*; *scale bars*, 100 μm) and mCherry-expressing axon terminals in the bed nucleus of the stria terminalis (*right*; *scale bars*, 1 mm) of vglut2-cre mice. (*C*) Coexpression of mCherry$^+$ neurons (*red*) and vglut2$^+$ neurons (*green*) in the paraventricular thalamus. *Scale bars*, 50 μm; *blue*, 4′,6-diamidino-2-phenylindole for nuclear staining. (*D* and *E*) Schematic diagrams of rabies virus–mediated monosynaptic tracing. (*F*) Representative images of the virus injection site and expression within the bed nucleus of the stria terminalis. Starter cells (*yellow*) coexpress avian tumor virus receptor A (TVA)-green fluorescent protein (*green*), rabies virus G, and rabies virus–EnvA-ΔG-DsRed (*red*) in the bed nucleus of the stria terminalis of vgat-Cre mice (*upper*) and vglut2-Cre (*lower*) mice. *Scale bars*, 100 μm. (*G*) Representative images of presynaptic cells in the paraventricular thalamus. Rabies

Chemogenetic Dissection Identification of the Paraventricular Thalamus Bed Nucleus of the Stria Terminalis Pathway

Previous studies have shown that paraventricular thalamus neurons are primarily glutamatergic neurons and are positive for VGLUT2 mRNA but not VGLUT1 mRNA.[33] To characterize contacts between the paraventricular thalamus and the bed nucleus of the stria terminalis, we first microinjected an adeno-associated virus expressing Cre-dependent channelrhodopsin-2 (AAV-DIO-ChR2-mCherry) into the paraventricular thalamus of vglut2-Cre mice (fig. 6, A to C). We observed that mCherry$^+$ glutamatergic cell bodies in the paraventricular thalamus and mCherry$^+$ fibers were mainly detected in the dorsolateral bed nucleus of the stria terminalis, as well as in other brain regions (fig. 6B; Supplemental Digital Content 1, fig. S4 [http://links.lww.com/ALN/C836]).

To further identify the cell type–specific connections between the paraventricular thalamus and the bed nucleus of stria terminalis neurons, we applied a Cre-dependent retrograde transmonosynaptic tracing tactic to ascertain the specific neuronal type of the bed nucleus of the stria terminalis that receives paraventricular thalamus excitatory projections (fig. 6D). Since glutamatergic and GABAergic neurons are typical and dominant cells in the bed nucleus of the stria terminalis, Cre-dependent helper viruses (AAV-EF1α-DIO-TVA-green fluorescent protein and AAV-EF1α-DIO-RVG) were microinjected into the bed nucleus of the stria terminalis of vglut2-Cre mice or vgat-Cre mice (fig. 6E). After 3 weeks, rabies virus (RV-ENVA-ΔG-dsRed) was microinjected into the same site and infected only the helper virus–positive neurons in the bed nucleus of the stria terminalis. Rabies virus could be transmitted retrogradely across monosynapses in the presence of these helper viruses. Glutamatergic or GABAergic neurons in the bed nucleus of the stria terminalis expressing both red and green fluorescent signals simultaneously were considered starter cells (fig. 6F). We observed intensely dsRed-labeled neurons in the paraventricular thalamus of vglut2-Cre mice and vgat-Cre mice (fig. 6G), suggesting that paraventricular thalamus neurons innervate glutamatergic and GABAergic neurons in the bed nucleus of the stria terminalis. Additionally, our immunofluorescence staining showed that the dsRed-labeled signal was largely colocalized with the vglut2 antibody signal (fig. 6, H and I), indicating that both GABAergic and glutamatergic neurons in the bed nucleus of the stria terminalis receive paraventricular thalamus glutamatergic projections directly. Only male mice were used in these experiments.

Fig. 6. (*Continued*) virus–labeled cells within the paraventricular thalamus of vgat-Cre mice (*left*) and vglut2-Cre (*right*) mice. *Scale bars*, 100 μm. (*H*) Identification of rabies virus–labeled neurons in the paraventricular thalamus. *White arrows* represent the colocalization of RV signals (*red*) and vglut2 antibody in vgat-Cre or vglut2-Cre mice. *Scale bars*, 50 μm. (*I*) Quantitation of the percentage of vglut2-expressing rabies virus–positive cells that projected onto the γ-aminobutyric acid–mediated and glutamatergic neurons in the bed nucleus of the stria terminalis (n = 4 for each group).

Chemogenetic Inhibition of the Paraventricular Thalamus Bed Nucleus of the Stria Terminalis Pathway Modulates Sevoflurane Anesthesia

To further verify the necessity of this specific pathway in regulating states of consciousness during sevoflurane anesthesia, retrograde transport Cre recombinase AAV_{retro}-Syn-Cre was bilaterally microinjected into the bed nucleus of the stria terminalis, and Cre-dependent AAV-EF1α-DIO-hM4D-mCherry or AAV-EF1α-DIO-mCherry was injected into the paraventricular thalamus for selective chemogenetic inhibition of paraventricular thalamus neurons that projected to the bed nucleus of the stria terminalis (fig. 7, A to C). We explored the effects on sevoflurane induction and emergence after the delivery of saline or clozapine *N*-oxide into hM4D-mCherry and mCherry (control) mice, respectively. The experiments were performed only in male mice. Our results showed that when exposed to 2.4% sevoflurane, the hM4D–clozapine *N*-oxide group showed a significant decrease in the induction time (87 ± 24 s) compared with that in the hM4D-saline group (136 ± 36 s, $P = 0.002$, n = 12; fig. 7D) and the mCherry–clozapine *N*-oxide group (124 ± 29 s, $P = 0.032$, n = 12; fig. 7D). The time to recovery of the righting reflex of sevoflurane anesthesia was prolonged in the hM4D–clozapine *N*-oxide group (292 ± 108 s) compared with that in the hM4D-saline group (174 ± 59 s, $P = 0.003$, n = 12; fig. 7E) and the mCherry–clozapine *N*-oxide group (160 ± 73 s, $P < 0.001$, n = 12; fig. 7E) after a 30-min exposure to 2.4% sevoflurane. The concentration at which 50% of the mice lost their righting reflex (EC_{50}) of sevoflurane was decreased in the hM4D–clozapine *N*-oxide group compared with that in the hM4D-saline group (1.13 [1.09 to 1.17] *vs.* 1.40 [1.36 to 1.44] vol%, n = 10; fig. 7F; Supplemental Digital Content 1, table S4 [http://links.lww.com/ALN/C836]) and the mCherry–clozapine *N*-oxide group (1.13 [1.09 to 1.17] *vs.* 1.42 [1.38 to 1.47] vol%, n = 10; fig. 7F; Supplemental Digital Content 1, table S4 [http://links.lww.com/ALN/C836]). The concentration at which 50% of the mice recovered their righting reflex (EC_{50}) of sevoflurane was also reduced in the hM4D–clozapine *N*-oxide group compared with that in the hM4D-saline group (1.03 [0.97 to 1.09] *vs.* 1.30 [1.26 to 1.35] vol%, n = 10; fig. 7G; Supplemental Digital Content 1, table S4 [http://links.lww.com/ALN/C836]) and the mCherry–clozapine *N*-oxide group (1.03 [0.97 to 1.09] *vs.* 1.33 [1.28 to 1.39] vol%, n = 10; fig. 7G; Supplemental Digital Content 1, table S4 [http://links.lww.com/ALN/C836]). Taken together, these results suggest that the suppression of the paraventricular

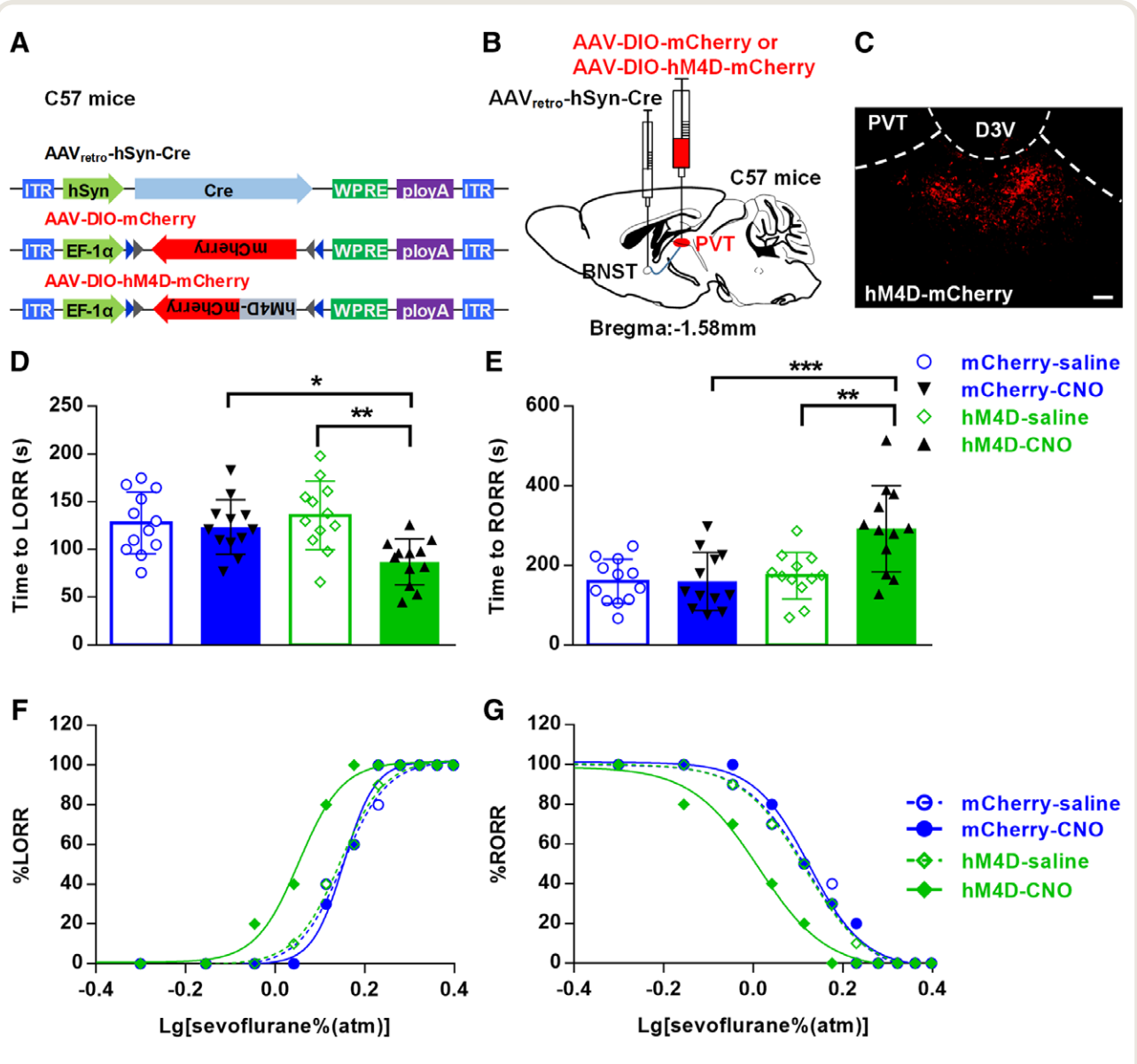

Fig. 7. The inhibition of the pathway from the paraventricular thalamus to the bed nucleus of the stria terminalis promoted induction and prolonged behavioral arousal from sevoflurane anesthesia. (*A* and *B*) Schematic representation of virus injection. AAV-DIO-hM4D-mCherry (or AAV-DIO-mCherry) was injected into the paraventricular thalamus, and AAV$_{retro}$-hSyn-Cre virus was injected into the bed nucleus of the stria terminalis. (*C*) Expression of hM4D-mCherry in neurons of the paraventricular thalamus that project to the bed nucleus of the stria terminalis. *Scale bar*, 100 μm. (*D* and *E*) Induction (*D*) and emergence (*E*) times with exposure to 2.4% sevoflurane (1 minimum alveolar concentration) in the inhibition group and the control group. The data are shown as the mean ± SD (one-way ANOVA). *$P < 0.05$; **$P < 0.01$; ***$P < 0.001$ (*post hoc* Bonferroni test, hM4D–clozapine *N*-oxide *vs.* hM4D-saline/mCherry–clozapine *N*-oxide, n = 12 for each group). (*F* and *G*) Dose–response curves of the loss of the righting reflex (*F*) and the recovery of the righting reflex (*G*) for the inhibition group and the control group.

thalamus bed nucleus of the stria terminalis pathway sped up the induction, delayed the recovery, and increased the sensitivity of sevoflurane anesthesia.

For cortical EEG activity, compared with saline injection, the inhibition of the paraventricular thalamus bed nucleus of the stria terminalis pathway in male mice led to an obvious increase in delta power during sevoflurane anesthesia induction (35.5 ± 3.8% *vs.* 47.2 ± 3.3%, $P < 0.0001$, n = 8; fig. 8, D and E) and emergence periods (39.4 ± 1.5% *vs.* 43.7 ± 2.6%, $P = 0.001$, n = 8; fig. 8, I and J), indicating that the paraventricular thalamus bed nucleus of the stria terminalis pathway could affect cortical sedation and arousal under sevoflurane anesthesia. Taken together, these results suggest that the paraventricular thalamus bed nucleus

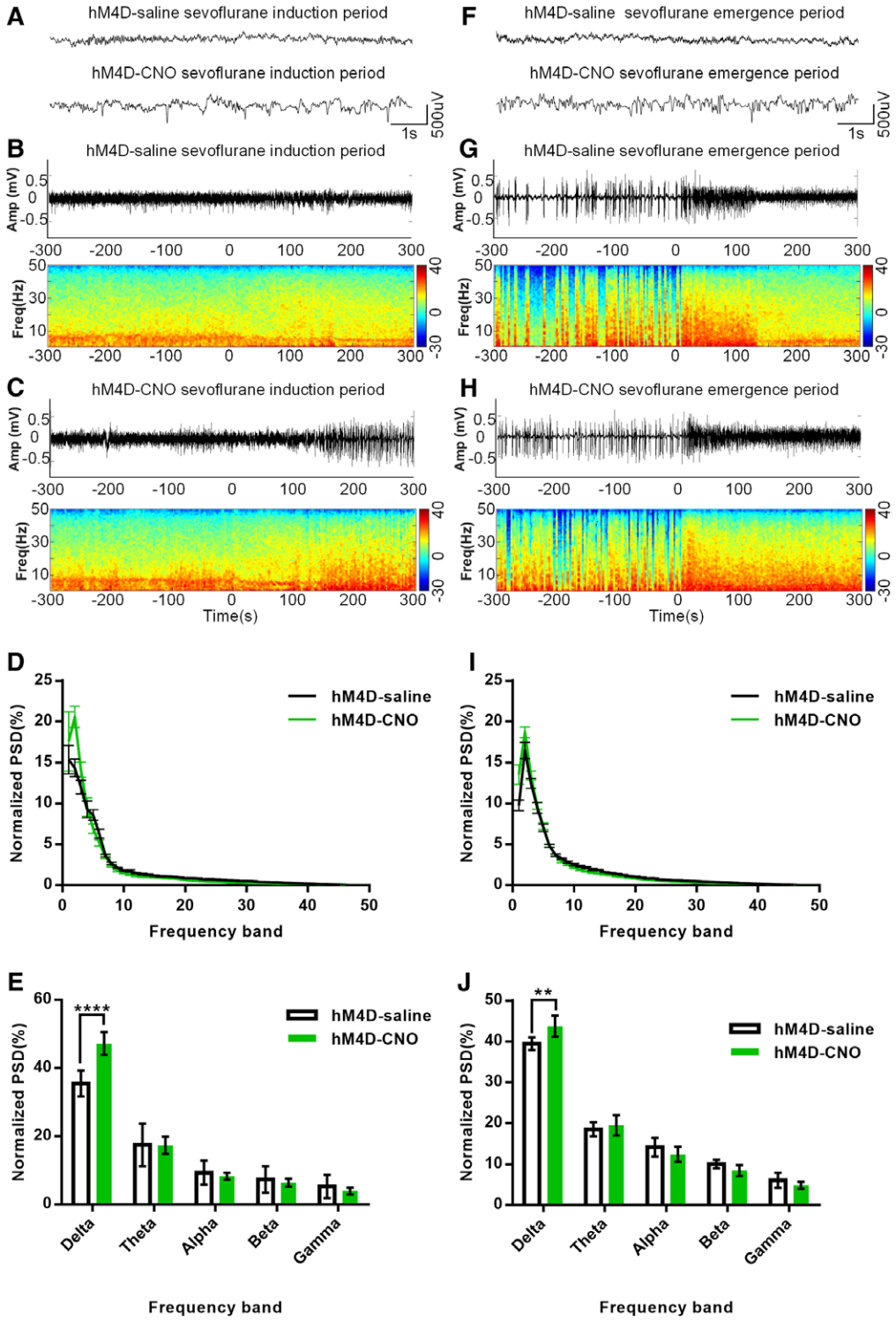

Fig. 8. The inhibition of the pathway from the paraventricular thalamus to the bed nucleus of the stria terminalis suppressed cortical electroencephalogram arousal during sevoflurane anesthesia. (*A*) Example of raw electroencephalogram traces during the induction period in hM4D mice after the delivery of clozapine *N*-oxide or saline. (*B* and *C*) Representative electroencephalogram power spectrograms of the suppression of the pathway from the paraventricular thalamus to the bed nucleus of the stria terminalis during the sevoflurane anesthesia induction period. Time zero on the timeline represents the initiation of sevoflurane anesthesia. (*D*) Normalized power spectral density changes during the sevoflurane induction period after intraperitoneal injection of saline or clozapine *N*-oxide (3 mg/kg). (*E*) Quantitative analysis of normalized power spectral density. Compared with saline, clozapine *N*-oxide induced a significant increase in the electroencephalogram delta power

of the stria terminalis pathway plays a vital role in sevoflurane anesthesia induction and emergence.

Optogenetic Activation of the Paraventricular Thalamus Bed Nucleus of the Stria Terminalis Pathway Modulates States of Consciousness during Sevoflurane Anesthesia

To further examine the role of projections from the paraventricular thalamus to the bed nucleus of the stria terminalis in sevoflurane anesthesia induction, maintenance, and emergence, we injected AAV-DIO-ChR2-mCherry or AAV-DIO-mCherry into the paraventricular thalamus of vglut2-Cre mice and then implanted optical fibers above the bed nucleus of the stria terminalis (fig. 9, A to C). We stimulated $PVT^{vglut2+}$ terminals in the bed nucleus of the stria terminalis with a 10-ms pulse width of blue light (473 nm) at 10 Hz in mice. Only male mice were used in this experiment.

Our results showed that the induction time in the ChR2-on group was significantly prolonged compared with that in the ChR2-off group (154 ± 24 s *vs.* 103 ± 36 s, $P = 0.012$, n = 8; fig. 9D) and the mCherry-on group (154 ± 24 s *vs.* 109 ± 33 s, $P = 0.034$, n = 8; fig. 9D). We also found that the emergence time in the ChR2-on group was significantly reduced compared with that in the ChR2-off group (107 ± 22 s *vs.* 169 ± 41 s, $P = 0.012$, n = 8; fig. 9E) and the mCherry-on group (107 ± 22 s *vs.* 160 ± 34 s, $P = 0.042$, n = 8; fig. 9E). All these results indicate that the paraventricular thalamus bed nucleus of the stria terminalis pathway may be the necessary pathway for the modulation of sevoflurane anesthesia induction and emergence.

Our results also showed that optical stimulation of $PVT^{vglut2+}$ terminals in the bed nucleus of the stria terminalis induced similar evidence of arousal behavior (fig. 9F; Supplemental Digital Content 1, table S6 [http://links.lww.com/ALN/C836]; Supplemental Digital Content 6, video S5 [http://links.lww.com/ALN/C841]), including leg, head, and tail movements (8 of 8), righting (5 of 8), and walking (3 of 8), in mice of the ChR2-on group during continuous steady-state general anesthesia with sevoflurane (Supplemental Digital Content 1, table S6 [http://links.lww.com/ALN/C836]), while this evident arousal behavior was barely seen in mice of the mCherry-on (Supplemental Digital Content 1, table S6 [http://links.lww.com/ALN/C836]; Supplemental Digital Content 7, video S6 [http://links.lww.com/ALN/C842]) or ChR2-off groups (Supplemental Digital Content 1, table S6 [http://links.lww.com/ALN/C836]). The Bayesian 95% CI for the difference in the propensity of righting at 10 Hz between the ChR2-on group and the mCherry-on group was 0.081 to 0.795 under sevoflurane continuous steady-state general anesthesia with the optostimulation of the paraventricular thalamus bed nucleus of the stria terminalis pathway (fig. 9, G and H). The posterior probability of the difference in righting between the two groups greater than 0 was 0.990, which was statistically significant (fig. 9H). In addition, the activation of the paraventricular thalamus bed nucleus of the stria terminalis projections caused a rapid increase in burst duration (fig. 10A; Supplemental Digital Content 8, video S7 [http://links.lww.com/ALN/C843]) and a significant increase in delta power compared with those observed prestimulation (fig. 10, C and D) and a significantly decreased burst-suppression ratio from 43.1 ± 10.4% to 2.8 ± 2.7% ($P < 0.001$, n = 8; fig. 10E) during sevoflurane-induced burst-suppression conditions, which was not seen in mCherry mice (fig. 10, F to J; Supplemental Digital Content 9, video S8 [http://links.lww.com/ALN/C844]). Our results indicate that the activation of the paraventricular thalamus bed nucleus of the stria terminalis pathway is sufficient to induce behavioral emergence during continuous steady-state general anesthesia with sevoflurane and rapidly reduce the depth of anesthesia during deep sevoflurane anesthesia.

Fig. 8. (*Continued*) of hM4D-expressing mice. The data are shown as the mean ± SD (two-way ANOVA). ****$P < 0.0001$ (*post hoc* Bonferroni test, hM4D–clozapine *N*-oxide *vs.* hM4D-saline, n = 8 for each group). (*F*) Representative raw electroencephalogram traces during the emergence period for the inhibition group and the control group. (*G* and *H*) Representative electroencephalogram power spectrograms during the sevoflurane anesthesia recovery period for the inhibition group (*green*) and control group (*black*). Zero on the timeline indicates the discontinuation of sevoflurane anesthesia. (*I*) Normalized power spectral density in the inhibition group (*green*) and control group (*black*) during the sevoflurane emergence period. (*J*) Quantitative analysis of normalized power spectral density shows that the suppression of the paraventricular thalamus bed nucleus of the stria terminalis pathway led to a significant increase in the delta power compared with that in the control mice during the recovery period. The data are shown as the mean ± SD (two-way ANOVA). **$P < 0.01$ (*post hoc* Bonferroni test, hM4D–clozapine *N*-oxide *vs.* hM4D-saline, n = 8 for each group).

Discussion

In the current study, we verified the regulatory effects of paraventricular thalamus glutamatergic neurons and the paraventricular thalamus bed nucleus of the stria terminalis pathway on sevoflurane-induced unconsciousness. Inhibition of paraventricular thalamus glutamatergic neurons or their pathways promoted the loss of consciousness and prolonged the recovery of consciousness, whereas activation induced opposite effects. Moreover, the cortical EEG activity during the induction and recovery periods of sevoflurane anesthesia was remarkably affected by the inhibition of paraventricular thalamus glutamatergic neurons or their pathways. Instantaneous optogenetic stimulation of paraventricular thalamus glutamatergic neurons or their pathways restored awake-like behavior during the maintenance period of light sevoflurane anesthesia and reduced the depth of anesthesia during sevoflurane-induced burst-suppression states.

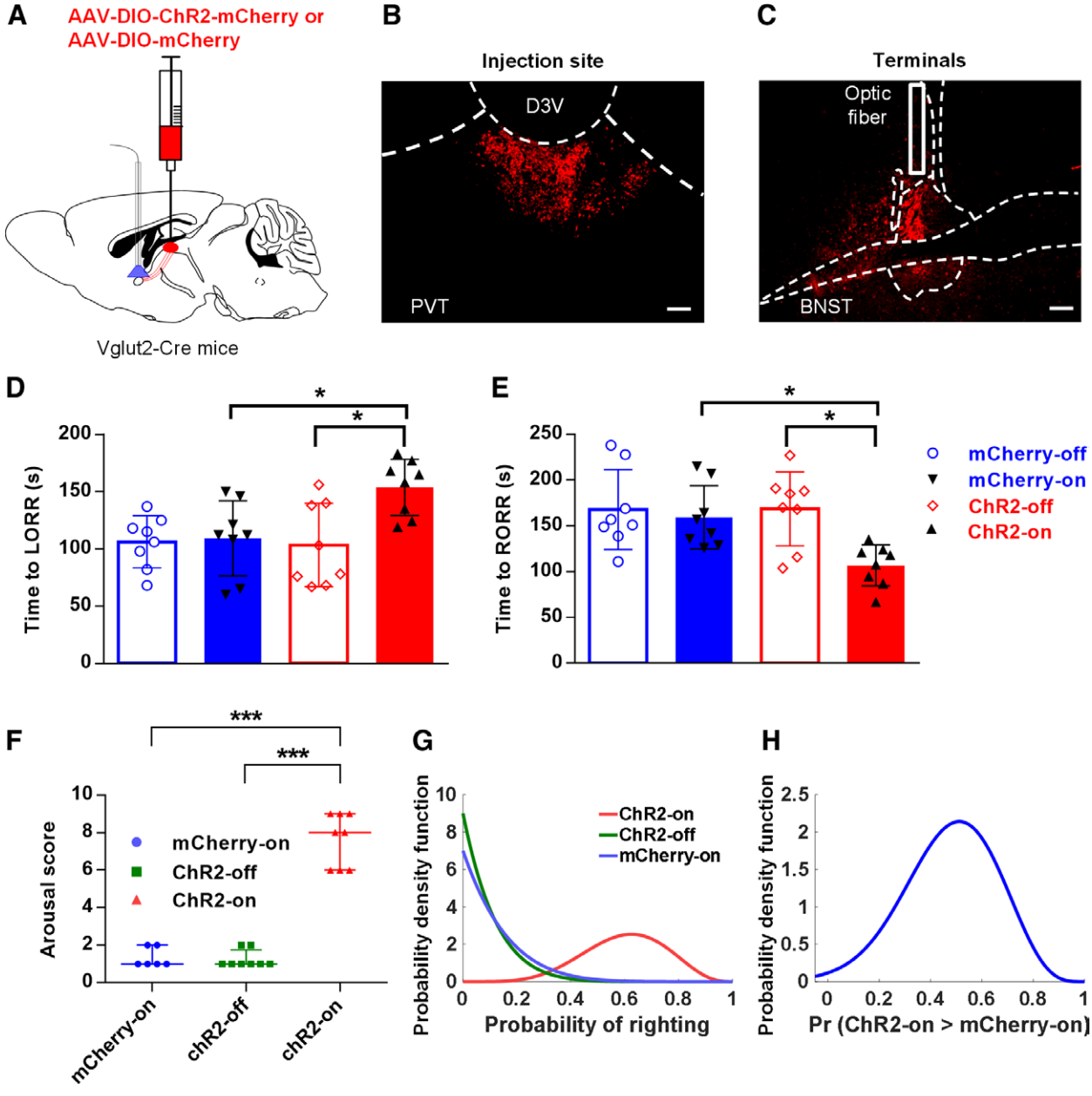

Fig. 9. Optogenetic activation of the paraventricular thalamus bed nucleus of the stria terminalis pathway delayed the induction, accelerated the emergence, and induced behavioral emergence during continuous steady-state general anesthesia with sevoflurane. (*A*) Schematic representation of virus injection and optical implantation. (*B* and *C*) Expression of AAV-DIO-ChR2-mCherry (*red*) in PVT$^{vglut2+}$ neurons (*B*) and mCherry containing vglut2^{+} terminals (*red*) in the bed nucleus of the stria terminalis (*C*). *Solid white lines* show the locations of optical fibers. *Scale bars*, 100 μm. (*D* and *E*) Results of the induction time (*D*) and emergence time (*E*) with exposure to 2.4% sevoflurane during the activation of the paraventricular thalamus bed nucleus of the stria terminalis pathway projections. The data are shown as the mean ± SD (one-way ANOVA). *$P < 0.05$ (*post hoc* Bonferroni test, hM4D–clozapine *N*-oxide *vs.* hM4D-saline/mCherry–clozapine *N*-oxide, n = 8 for each group). (*F*) Total arousal response score for the optical stimulation of the paraventricular thalamus bed nucleus of the stria terminalis pathway (10-ms pulses, 10 Hz, 120 s) during continuous steady-state general anesthesia with 1.4 to 1.5% sevoflurane. The data are reported as the median and interquartile range (25th, 75th). ***$P < 0.001$ (n = 8 in the ChR2-on/off group, and n = 6 in the mCherry-on group). (*G*) Posterior densities for the propensity of righting for the ChR2-on (*red*), ChR2-off (*green*), and mCherry-on (*blue*) groups during optical stimulation of the paraventricular thalamus bed nucleus of the stria terminalis pathway. Posterior densities are obtained from beta distributions. (*H*) Posterior probability of the difference between the ChR2-on group and the mCherry-on group during optical stimulation of the paraventricular thalamus bed nucleus of the stria terminalis pathway under continuous steady-state general anesthesia with sevoflurane.

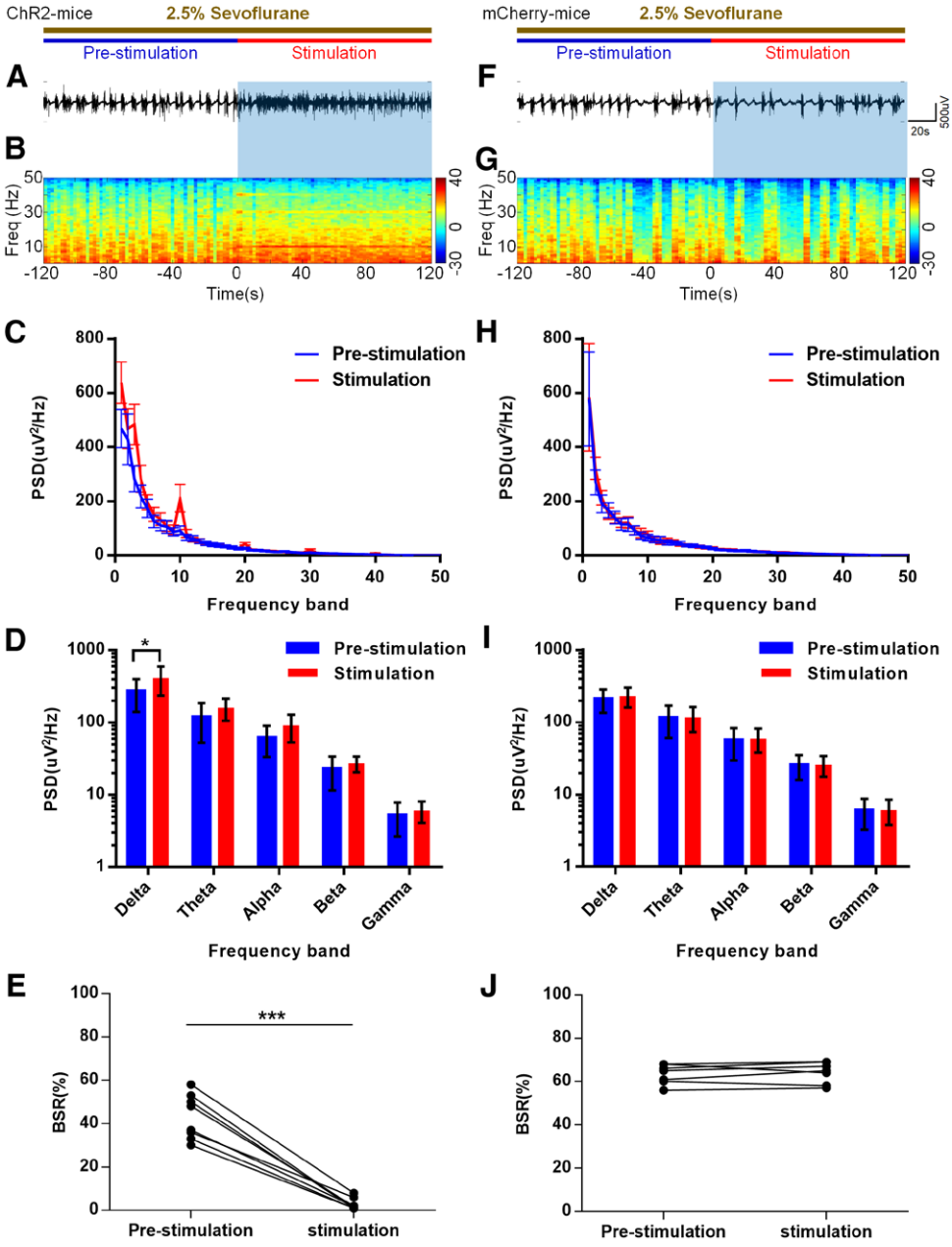

Fig. 10. Optogenetic activation of the paraventricular thalamus bed nucleus of the stria terminalis pathway reduced the depth of anesthesia during sevoflurane-induced burst-suppression conditions. (*A*) Example raw electroencephalogram traces and electroencephalogram power spectra (*B*) in vglut2-cre mice injected with AAV-DIO-ChR2-mCherry. *Blue shading* represents the light stimulation period (10-ms pulses; 10 Hz; 120 s). Time zero indicates the beginning of light stimulation during burst suppression conditions induced by 2.5% sevoflurane. (*C*) Average power spectral density in the stimulation of the paraventricular thalamus bed nucleus of the stria terminalis pathway computed from 120 s before stimulation (*blue*) to 120 s during optical stimulation (*red*). (*D*) Quantitative analysis of the average power spectral density between the prestimulation and stimulation periods in the stimulation of the paraventricular thalamus bed nucleus of the stria terminalis pathway in mice. $^{*}P < 0.05$ (n = 8 for each group). (*E*) Effect of the activation of the paraventricular thalamus bed nucleus of the stria terminalis pathway on the electroencephalogram burst-suppression ratio during continuous sevoflurane anesthesia. $^{***}P < 0.001$ (n = 8 for each group). (*F* and *G*) Typical examples of electroencephalogram traces (*F*) and electroencephalogram power spectra (*G*) in the control group (vglut2-cre mice injected with AAV-DIO-mCherry). (*H*) Average power spectral density in the control group computed from 120 s before stimulation (*blue*) to 120 s after optical stimulation (*red*). (*I*) Quantitative analysis of the average power spectral density between the prestimulation and stimulation periods in the control group. (*J*) Effect of optical stimulation on the electroencephalogram burst-suppression ratio during continuous sevoflurane anesthesia in the control group ($P = 0.527$, n = 7 for each group).

Recent studies have demonstrated that the central medial thalamus is the key hub for initiating sleep or anesthetic-induced unconsciousness.[34] Patients with local lesions in the paramedian region of the thalamus showed disturbances of consciousness.[35] Alkire *et al.*[36] found that local injection of nicotine, a cholinergic nicotinic receptor agonist, into the central medial thalamus could reverse sevoflurane-induced loss of the righting reflex. Ren *et al.*[15] found that optogenetic activation of the paraventricular thalamus promoted emergence from isoflurane anesthesia. In concordance with previous studies, we verified that paraventricular thalamus glutamatergic neurons can greatly affect the general anesthesia emergence time. It is generally believed that emergence from general anesthesia is the reverse of the process of induction, caused by the passive elimination of anesthetic drugs at the site of action in the central nervous system. However, recent studies have shown that the neural substrates mediating induction and emergence are not consistent.[4] Emerging evidence suggests that anesthetic-induced loss of consciousness is related to the disruption of corticocortical or thalamocortical functional connections, while recovery from anesthesia is mostly controlled by ascending arousal pathways involved in sleep–wakefulness.[37,38] In contrast to a previous study, inhibition of the dopaminergic pathway of the paraventricular thalamus prolonged the isoflurane anesthesia recovery time but had no significant effect on the induction time.[39] We found that the sevoflurane anesthesia induction time and recovery time were both significantly affected by the paraventricular thalamus. Our results suggest that there are shared neural circuits involved in the process of regulating the sevoflurane-induced loss and recovery of consciousness.

There is robust evidence of an association between EEG oscillations in the frontal cortex and anesthetic-induced loss of consciousness.[3,40] Recent evidence suggests that the delta power is a reliable predictor of transitions between consciousness and unconsciousness under anesthesia. Delta activity is a typical signature of unconsciousness.[40,41] Our results showed that the delta power was affected by the paraventricular thalamus bed nucleus of the stria terminalis pathway during the period of sevoflurane induction. Delta oscillations during anesthesia resulted from a pronounced hyperpolarization of thalamocortical relay neurons caused by complete withdrawal of excitatory aminergic inputs.[42] Therefore, our results suggested that the inhibition of the paraventricular thalamus or its pathways during sevoflurane anesthesia could exacerbate hyperpolarization and accelerate the synchronized activity of the cerebral cortex, thereby promoting the loss of consciousness. Furthermore, during the sevoflurane emergence period, we found that the inhibition of the paraventricular thalamus increased the delta power and decreased the theta power. Theta waves are associated with attention as an element of some forms of exploratory behavior and of the process of dream formation and expression, both of which are characterized by consciousness.[43] Our results suggested that a reduction in theta power, combined with an increase in sleep-related delta oscillatory activity, might contribute to the delay in the recovery of consciousness. The difference in EEG results between the induction and recovery periods also indicates that the regulatory mechanism of paraventricular thalamus glutamatergic neurons during sevoflurane-induced loss and recovery of consciousness may be different.

Furthermore, inhibition of the paraventricular thalamus bed nucleus of the stria terminalis pathway significantly increased only the delta power, without affecting the theta power, during the sevoflurane emergence period, suggesting that this pathway may be one of the nerve loops mediating the arousal-promoting effect of the paraventricular thalamus. Recent studies have found that neurons expressing dopamine D1 receptor in the nucleus accumbens played a significant role in wakefulness, and the stimulation of these neurons at 20 or 30 Hz regulated the state of consciousness in sevoflurane anesthesia.[28,44] Ren *et al.*[15] reported that the activation of paraventricular thalamus-nucleus accumbens projections promoted the sleep–wake transition. However, Hua *et al.*[25] found that photogenetic activation of the paraventricular thalamus-nucleus accumbens pathway at 5 Hz had no obvious arousal effect. The differences in these findings may be due to differences in the frequency of the stimulation, and it was also reasoned that high-frequency stimulation may cause retrograde activation.[25] Thus, whether the paraventricular thalamus-nucleus accumbens is involved in the regulation of sevoflurane-induced unconsciousness remains unclear.

Burst suppression is observed in various pathologic conditions, including deep general anesthesia, hypoxia-induced deep coma, hypothermia, and childhood encephalopathies, and is often accompanied by a profound obliteration of consciousness.[45] Recent studies have demonstrated that sevoflurane-induced unconsciousness during burst-suppression conditions results from the disruption of functional connectivity between frontal and thalamic networks.[46] It was also reported that anesthetic-induced burst suppression calls for glutamate-mediated excitatory synaptic transmission and that EEG burst activities can be evoked by barrages of glutamate-mediated excitatory events in intrinsic neocortical circuitry.[47] Similar to previous studies,[15] we found that optical stimulation of the paraventricular thalamus bed nucleus of the stria terminalis pathway increased burst duration and burst frequency and decreased the burst-suppression ratio during anesthetic-induced burst-suppression states, suggesting that EEG bursts could be triggered by excitatory events in the paraventricular thalamus glutamatergic neurons and its network. Most EEG arousal represents the transition from mixed high-amplitude slow activity to higher-frequency low-amplitude activity. However, there is a paradoxical delta arousal; that is, the power in the delta band (0.5 to 4 Hz) is increased. Our results showed that optical stimulation of the paraventricular thalamus bed

nucleus of the stria terminalis pathway induced an increase in the delta band during sevoflurane-induced burst suppression. This paradoxical phenomenon has also been observed in the activation of histaminergic transmission in the basal forebrain, and the administration of histamine in the basal forebrain could shift neocortical electroencephalography from a burst-suppression pattern to delta activity, suggesting that EEG delta arousal was induced by histaminergic transmission during deep isoflurane anesthesia.[12] Delta arousal has also been shown to occur when a patient is exposed to noxious stimulation with inadequate analgesia under deep anesthesia.[48] It has also been suggested that the increase in delta power could be induced by high-frequency midbrain reticular stimulation in anesthetized cats.[49] While termed delta arousal, these delta responses may not necessarily imply the progression toward the restoration of consciousness.[48] In our experiments, the delta power and burst duration were increased after optical stimulation, suggesting cortical activation and a decrease in anesthesia depth, but we did not conclude that consciousness was restored after stimulation of the paraventricular thalamus during deep anesthesia with burst suppression. Another unexpected finding was that the activation of the paraventricular thalamus bed nucleus of the stria terminalis pathway was sufficient to induce behavioral arousal during light sevoflurane anesthesia maintenance, which was not seen in isoflurane anesthesia.[15] This difference may be attributed to the different affinities of isoflurane and sevoflurane for the same molecule or receptor in the paraventricular thalamus[1,50] and suggests that the potential neural circuit mechanism of the two anesthetics may not be exactly the same.

However, there are still some limitations of our study. First, whether there are sex differences in the effect of the paraventricular thalamus bed nucleus of the stria terminalis pathway on anesthetic arousal still needs to be further explored. Second, we identified only the cell types of neurons in the bed nucleus of the stria terminalis innervated by paraventricular thalamus glutamatergic neurons, and the functional connections of the paraventricular thalamus bed nucleus of the stria terminalis pathway need to be further characterized. We speculate that the arousal-promoting effect of paraventricular thalamus glutamatergic neurons may be directly mediated by GABAergic neurons in the bed nucleus of the stria terminalis. However, it is not known whether there is a local loop between glutamatergic and GABAergic neurons in the bed nucleus of the stria terminalis, and whether paraventricular thalamus glutamatergic neurons can indirectly activate the GABAergic neurons in the bed nucleus of the stria terminalis through this local loop and then play a role in promoting the arousal effect of sevoflurane anesthesia still needs to be further investigated. Finally, experiments on off-target injections would further enhance the study.

In summary, our findings support the hypothesis that paraventricular thalamus glutamatergic neurons play a significant role in modulating states of consciousness during sevoflurane anesthesia by directly projecting to the bed nucleus of the stria terminalis. Improved general anesthetic drugs should satisfy the desirable outcomes, such as surgery without pain, awareness, or memory, and minimize undesirable results, such as anesthesia-associated delirium, cardiovascular depression, and death. Understanding the neural basis of general anesthesia will facilitate the development of new anesthetics.

Acknowledgments

The authors thank Haohong Li, Ph.D. (Wuhan National Laboratory for Optoelectronics, Huazhong University of Science and Technology, Hubei, China), for providing vglut2-Cre and vgat-Cre mice, and Pengcheng Huang, Ph.D. (Wuhan National Laboratory for Optoelectronics, Huazhong University of Science and Technology), for technical support, and Xinfeng Chen, Ph.D. (Chinese Institute for Brain Research, Beijing, China), for technical support.

Research Support

Supported by grant Nos. 82071556 and 81873793 from the National Natural Science Foundation of China (Beijing, China).

Competing Interests

The authors declare no competing interests.

Correspondence

Address correspondence to Dr. Mei: Tongji Hospital, Tongji Medical College, Huazhong University of Science and Technology, Jiefang Avenue 1095, Wuhan 430030, China. wmei@hust.edu.cn.

References

1. Franks NP: General anaesthesia: From molecular targets to neuronal pathways of sleep and arousal. Nat Rev Neurosci 2008; 9:370–86
2. Kelz MB, Mashour GA: The biology of general anesthesia from paramecium to primate. Curr Biol 2019; 29:R1199–210
3. Hemmings HC Jr, Riegelhaupt PM, Kelz MB, Solt K, Eckenhoff RG, Orser BA, Goldstein PA: Towards a comprehensive understanding of anesthetic mechanisms of action: A decade of discovery. Trends Pharmacol Sci 2019; 40:464–81
4. Kelz MB, Sun Y, Chen J, Cheng Meng Q, Moore JT, Veasey SC, Dixon S, Thornton M, Funato H, Yanagisawa M: An essential role for orexins in emergence from

general anesthesia. Proc Natl Acad Sci U S A 2008; 105:1309–14
5. Wang TX, Xiong B, Xu W, Wei HH, Qu WM, Hong ZY, Huang ZL: Activation of parabrachial nucleus glutamatergic neurons accelerates reanimation from sevoflurane anesthesia in mice. Anesthesiology 2019; 130:106–18
6. Yin L, Li L, Deng J, Wang D, Guo Y, Zhang X, Li H, Zhao S, Zhong H, Dong H: Optogenetic/chemogenetic activation of GABAergic neurons in the ventral tegmental area facilitates general anesthesia via projections to the lateral hypothalamus in mice. Front Neural Circuits 2019; 13:73
7. Vazey EM, Aston-Jones G: Designer receptor manipulations reveal a role of the locus coeruleus noradrenergic system in isoflurane general anesthesia. Proc Natl Acad Sci U S A 2014; 111:3859–64
8. Hu FY, Hanna GM, Han W, Mardini F, Thomas SA, Wyner AJ, Kelz MB: Hypnotic hypersensitivity to volatile anesthetics and dexmedetomidine in dopamine β-hydroxylase knockout mice. Anesthesiology 2012; 117:1006–17
9. Luo T, Leung LS: Involvement of tuberomamillary histaminergic neurons in isoflurane anesthesia. Anesthesiology 2011; 115:36–43
10. Taylor NE, Van Dort CJ, Kenny JD, Pei J, Guidera JA, Vlasov KY, Lee JT, Boyden ES, Brown EN, Solt K: Optogenetic activation of dopamine neurons in the ventral tegmental area induces reanimation from general anesthesia. Proc Natl Acad Sci U S A 2016; 113:12826–31
11. Solt K, Van Dort CJ, Chemali JJ, Taylor NE, Kenny JD, Brown EN: Electrical stimulation of the ventral tegmental area induces reanimation from general anesthesia. Anesthesiology 2014; 121:311–9
12. Luo T, Leung LS: Basal forebrain histaminergic transmission modulates electroencephalographic activity and emergence from isoflurane anesthesia. Anesthesiology 2009; 111:725–33
13. Moore JT, Chen J, Han B, Meng QC, Veasey SC, Beck SG, Kelz MB: Direct activation of sleep-promoting VLPO neurons by volatile anesthetics contributes to anesthetic hypnosis. Curr Biol 2012; 22:2008–16
14. Gelegen C, Miracca G, Ran MZ, Harding EC, Ye Z, Yu X, Tossell K, Houston CM, Yustos R, Hawkins ED, Vyssotski AL, Dong HL, Wisden W, Franks NP: Excitatory pathways from the lateral habenula enable propofol-induced sedation. Curr Biol 2018; 28:580–7.e5
15. Ren S, Wang Y, Yue F, Cheng X, Dang R, Qiao Q, Sun X, Li X, Jiang Q, Yao J, Qin H, Wang G, Liao X, Gao D, Xia J, Zhang J, Hu B, Yan J, Wang Y, Xu M, Han Y, Tang X, Chen X, He C, Hu Z: The paraventricular thalamus is a critical thalamic area for wakefulness. Science 2018; 362:429–34
16. Liang SH, Yin JB, Sun Y, Bai Y, Zhou KX, Zhao WJ, Wang W, Dong YL, Li YQ: Collateral projections from the lateral parabrachial nucleus to the paraventricular thalamic nucleus and the central amygdaloid nucleus in the rat. Neurosci Lett 2016; 629:245–50
17. Otake K, Ruggiero DA, Nakamura Y: Adrenergic innervation of forebrain neurons that project to the paraventricular thalamic nucleus in the rat. Brain Res 1995; 697:17–26
18. Hsu DT, Price JL: Paraventricular thalamic nucleus: Subcortical connections and innervation by serotonin, orexin, and corticotropin-releasing hormone in macaque monkeys. J Comp Neurol 2009; 512:825–48
19. Lee JS, Lee EY, Lee HS: Hypothalamic, feeding/arousal-related peptidergic projections to the paraventricular thalamic nucleus in the rat. Brain Res 2015; 1598:97–113
20. Otis JM, Namboodiri VM, Matan AM, Voets ES, Mohorn EP, Kosyk O, McHenry JA, Robinson JE, Resendez SL, Rossi MA, Stuber GD: Prefrontal cortex output circuits guide reward seeking through divergent cue encoding. Nature 2017; 543:103–7
21. Li S, Kirouac GJ: Projections from the paraventricular nucleus of the thalamus to the forebrain, with special emphasis on the extended amygdala. J Comp Neurol 2008; 506:263–87
22. Crone JS, Lutkenhoff ES, Bio BJ, Laureys S, Monti MM: Testing proposed neuronal models of effective connectivity within the cortico-basal ganglia-thalamo-cortical loop during loss of consciousness. Cereb Cortex 2017; 27:2727–38
23. Lebow MA, Chen A: Overshadowed by the amygdala: The bed nucleus of the stria terminalis emerges as key to psychiatric disorders. Mol Psychiatry 2016; 21:450–63
24. Kodani S, Soya S, Sakurai T: Excitation of GABAergic neurons in the bed nucleus of the stria terminalis triggers immediate transition from non-rapid eye movement sleep to wakefulness in mice. J Neurosci 2017; 37:7164–76
25. Hua R, Wang X, Chen X, Wang X, Huang P, Li P, Mei W, Li H: Calretinin neurons in the midline thalamus modulate starvation-induced arousal. Curr Biol 2018; 28:3948–59.e4
26. Yang Y, Liu DQ, Huang W, Deng J, Sun Y, Zuo Y, Poo MM: Selective synaptic remodeling of amygdalocortical connections associated with fear memory. Nat Neurosci 2016; 19:1348–55
27. Sun Y, Chen J, Pruckmayr G, Baumgardner JE, Eckmann DM, Eckenhoff RG, Kelz MB: High throughput modular chambers for rapid evaluation of anesthetic sensitivity. BMC Anesthesiol 2006; 6:13
28. Bao WW, Xu W, Pan GJ, Wang TX, Han Y, Qu WM, Li WX, Huang ZL: Nucleus accumbens neurons expressing dopamine D1 receptors modulate states

of consciousness in sevoflurane anesthesia. Curr Biol 2021; 31:1893–902.e5
29. Du H, Deng W, Aimone JB, Ge M, Parylak S, Walch K, Zhang W, Cook J, Song H, Wang L, Gage FH, Mu Y: Dopaminergic inputs in the dentate gyrus direct the choice of memory encoding. Proc Natl Acad Sci U S A 2016; 113:E5501–10
30. Arena A, Lamanna J, Gemma M, Ripamonti M, Ravasio G, Zimarino V, De Vitis A, Beretta L, Malgaroli A: Linear transformation of the encoding mechanism for light intensity underlies the paradoxical enhancement of cortical visual responses by sevoflurane. J Physiol 2017; 595:321–39
31. Chemali JJ, Wong KF, Solt K, Brown EN: A state-space model of the burst suppression ratio. Annu Int Conf IEEE Eng Med Biol Soc 2011; 2011:1431–4
32. McCarren HS, Moore JT, Kelz MB: Assessing changes in volatile general anesthetic sensitivity of mice after local or systemic pharmacological intervention. J Vis Exp 2013; 80: e51079
33. Liang SH, Zhao WJ, Yin JB, Chen YB, Li JN, Feng B, Lu YC, Wang J, Dong YL, Li YQ: A neural circuit from thalamic paraventricular nucleus to central amygdala for the facilitation of neuropathic pain. J Neurosci 2020; 40:7837–54
34. Baker R, Gent TC, Yang Q, Parker S, Vyssotski AL, Wisden W, Brickley SG, Franks NP: Altered activity in the central medial thalamus precedes changes in the neocortex during transitions into both sleep and propofol anesthesia. J Neurosci 2014; 34:13326–35
35. Kundu B, Brock AA, Englot DJ, Butson CR, Rolston JD: Deep brain stimulation for the treatment of disorders of consciousness and cognition in traumatic brain injury patients: A review. Neurosurg Focus 2018; 45:E14
36. Alkire MT, McReynolds JR, Hahn EL, Trivedi AN: Thalamic microinjection of nicotine reverses sevoflurane-induced loss of righting reflex in the rat. Anesthesiology 2007; 107:264–72
37. Voss LJ, García PS, Hentschke H, Banks MI: Understanding the effects of general anesthetics on cortical network activity using *ex vivo* preparations. Anesthesiology 2019; 130:1049–63
38. Akeju O, Loggia ML, Catana C, Pavone KJ, Vazquez R, Rhee J, Contreras Ramirez V, Chonde DB, Izquierdo-Garcia D, Arabasz G, Hsu S, Habeeb K, Hooker JM, Napadow V, Brown EN, Purdon PL: Disruption of thalamic functional connectivity is a neural correlate of dexmedetomidine-induced unconsciousness. Elife 2014; 3:e04499
39. Ao Y, Yang B, Zhang C, Li S, Xu H: Application of quinpirole in the paraventricular thalamus facilitates emergence from isoflurane anesthesia in mice. Brain Behav 2021; 11:e01903
40. Mashour GA, Avidan MS: Black swans: Challenging the relationship of anaesthetic-induced unconsciousness and electroencephalographic oscillations in the frontal cortex. Br J Anaesth 2017; 119:563–5
41. Lee M, Sanders RD, Yeom SK, Won DO, Seo KS, Kim HJ, Tononi G, Lee SW: Network properties in transitions of consciousness during propofol-induced sedation. Sci Rep 2017; 7:16791
42. Brown RE, Basheer R, McKenna JT, Strecker RE, McCarley RW: Control of sleep and wakefulness. Physiol Rev 2012; 92:1087–187
43. Valle AC, Timo-Iaria C, Fraga JL, Sameshima K, Yamashita R: Theta waves and behavioral manifestations of alertness and dreaming activity in the rat. Braz J Med Biol Res 1992; 25:745–9
44. Luo YJ, Li YD, Wang L, Yang SR, Yuan XS, Wang J, Cherasse Y, Lazarus M, Chen JF, Qu WM, Huang ZL: Nucleus accumbens controls wakefulness by a subpopulation of neurons expressing dopamine D1 receptors. Nat Commun 2018; 9:1576
45. Amzica F: What does burst suppression really mean? Epilepsy Behav 2015; 49:234–7
46. Ranft A, Golkowski D, Kiel T, Riedl V, Kohl P, Rohrer G, Pientka J, Berger S, Thul A, Maurer M, Preibisch C, Zimmer C, Mashour GA, Kochs EF, Jordan D, Ilg R: Neural correlates of sevoflurane-induced unconsciousness identified by simultaneous functional magnetic resonance imaging and electroencephalography. Anesthesiology 2016; 125:861–72
47. Lukatch HS, Kiddoo CE, Maciver MB: Anesthetic-induced burst suppression EEG activity requires glutamate-mediated excitatory synaptic transmission. Cereb Cortex 2005; 15:1322–31
48. García PS, Kreuzer M, Hight D, Sleigh JW: Effects of noxious stimulation on the electroencephalogram during general anaesthesia: A narrative review and approach to analgesic titration. Br J Anaesth 2021; 126:445–57
49. Kaada BR, Thomas F, Alnaes E, Wester K: EEG synchronization induced by high frequency midbrain reticular stimulation in anesthetized cats. Electroencephalogr Clin Neurophysiol 1967; 22:220–30
50. Kim D, Kim HJ, Ahn S: Anesthetics mechanisms: A review of putative target proteins at the cellular and molecular level. Curr Drug Targets 2018; 19:1333–43